EFEE

NEWSLETTER

In this edition:

A new class of cryogenic Liquid Oxygen Explosives

Borehole Deviation Control Using Electronics: An Euler's Approach

Ready-to-use satellite based subsidence detection of geo-hazards, infrastructure and mining sites

...and much more!

EFEE

10th ANNIVERSARY WORLD CONFERENCE

HELSINKI 2019

INFRA

10th ANNIVERSARY

Scandic Marina Congress Center, Helsinki | 15th - 18th September 2019

NEWSLETTER

February 2019

We in EFEE hope you will enjoy the present EFEE-Newsletter. The next edition will be published in May 2019. Please feel free to contact the EFEE secretariat or write to newsletter@efee.eu in case:

- You have a story you want to bring in the Newsletter
- You have a future event for the next EFEE Newsletter upcoming events list
- You want to advertise in an upcoming Newsletter edition

or any other matter.

Doru Anghelache, Chairman of the Newsletter Committee and the Vice President of EFEE

and Teele Tuuna, Editor of EFEE Newsletter - newsletter@efee.eu

EFEE

EFEE SECRETARY GENERAL
ROGER HOLMBERG, JÄRNGRUVEVÄGEN 6
618 92 KOLMÅRDEN, SWEDEN
newsletter@efee.eu
www.efee.eu

Dear EFEE members, the President´s voice

I welcome you all to read the first EFEE Newsletter of 2019! I hope that you will find some of the technical articles interesting as there are 4 of them included this time – all very different from each other but describing important technical development in various fields of our trade.

The recent winter period has been extraordinary busy. The business is good and vibrant but I have pushed my calendar and attended also several brilliant trade conferences since the last issue.

In the end of November I attended the traditional Fjellsprengnings-konferansen "Rock blasting conference" in Oslo – the main trade event of the year arranged by Norwegian Tunneling society and Norwegian Geotechnical society. This annual event was participated by around 1200 delegates and 30 exhibitors this year.

Mid January we had the semi-annual conference on "Rock excavation and technique" in Helsinki Finland. This conference had approximately 200 delegates and 10 exhibitors which is also more than average. There were 20 papers presented during 1 and a half days, most of them from Finland but also some international. Needless to say the networking was extremely vibrant during brakes and the festive dinner as all these professionals met a lot of old and also some new friends and colleagues and exchanged their thoughts. The program this year was one of the most interesting ever.

In the end of January I had the chance to visit the two-day annual conference in Stockholm Sweden where over 200 professionals met at the 21st Bergsprängardagarna – "shotfirers days". There was also around 10 exhibitors in place. I must say that this conference always has some very interesting and brilliant presentations and so it did also this year! Unfortunately they are mostly in Swedish so I cannot recommend the event to EFEE members coming from outside Northern Europe.

I then travelled to Nashville, USA to attend the 45th annual ISEE conference straight after returning from Stockholm. That was a bit hard but very rewarding as I got a chance to interact with over 1800 delegates and hundreds of exhibitors that were attending the conference this year. I had a special mission to attract exhibitors and authors to EFEE Helsinki conference and I was pleased to note that most people I talked to had already decided to join our next conference in Europe. Therefore we can expect several good technical papers presented by most recognized experts in North America as well as many of our usual and some new exhibitors from the same region. It feels like EFEE conferences have been established as one of the major international events of the year and are not to be missed even if the distance to travel might be long. I am glad and proud that we have reached this status and this is of course achieved by the hard work put into the previous 9 conferences.

I am extremely happy to announce that we have received a large number of paper proposals for the 10th EFEE conference which will be held in Helsinki in September. The selection of papers is on its way as we speak and I am convinced that our extremely experienced and skilful technical committee will be able to find and choose a full plate of superb technical papers for you to hear in Helsinki.

The arrangement of the conference is also proceeding well and most details are soon in place. There will be a pre-conference work shop available on Sunday where the theme will be about effective blasting works in sensitive urban surrounding. There is a tour in conjunction with the work shop which will take participants to see some of many underground spaces underneath city centre of Helsinki. Welcome reception on Sunday will be hosted by the city of Helsinki. Actual conference and exhibition days will be Monday and Tuesdays as usual. We are expecting the exhibition to sell out as normal even though we have some more space available this year. The interest towards exhibition space has been enormous.

This year there will also be a full day post conference tour available on Wednesday. This tour will take limited number of guests to the only working dynamite factory in Norther Europe as well as to a mining museum located in conjunction to the oldest working underground mine in Finland. Discussions are in place to include also a visit to the working mine and I am hopeful to be able to arrange this as well.

Since this will be the 10th conference there are of course a lot of extraordinary arrangements planned for you! I am looking forward to meeting many of you in Helsinki 15-18 of September!

Before Helsinki there will be a possibility to attend the PECCS multiplier event in Berlin on 27th of March. This meeting is aimed to all European authorities and trainers working with certification of shotfirers. In this meeting you will be presented the PECCS training system including the Guidebook and Online Learning Environment developed to support the training. Please see the PECCS site www.shotfirer.eu for more information.

I wish you will enjoy reading this use of Newsletter and that you will have a nice spring with lots of successful blasting experiences.

Jari Honkanen, President of EFEE

A new class of cryogenic Liquid Oxygen Explosives

1. Introduction

The INBT (Institute of New Basic Technology) developed a new class of cryogenic Liquid Oxygen Explosives (called LOX-Ex). Based on LOX-Ex the INBT developed new technologies [1], [2] and [3].

The LOX-Ex technologies serve the purpose to make highest chemical energy and power densities accessible for industrial applications in dimensions that were not yet available for processes of rock fragmentation and material processing. With that technology it is possible to fragment, to pulverise, or just to destroy rocks in a controlled way. It is also possible to produce diamonds or diamond powder. With the LOX-Ex technology it was worldwide to the first time possible to create intermetallic compounds of otherwise inert metals, such as tungsten carbide with stainless steel. The LOX-Ex technologies also could be used to shape complex objects in a fast, inexpensive, environmentally-sensitive and environmentally-friendly way.

This class of cryogenic explosives consists out of finest molecular structured nanoparticles of a substance as fuel and liquid oxygen (LOX).

This combination delivers highest chemical energy and power density. It opens new perspectives for the automated industrial production, and in the field of mining, tunnelling, and excavation with LOX-Ex in an automated way.

Using the LOX-Ex technologies guaranties a new safety concept, there are no residual explosives, no noxious fumes or toxic gases, and the swaths are nitrogen oxide-free. The LOX-Ex technologies are very cost efficient.

1.1 Advantages of LOX-Ex

The following materials were successfully used in the LOX-Ex technologies:

- Polymethylmethacrylat (PMMA),
- Polystyrene (PS),
- Polypropylene (PP) and
- Various metallic fuels (such as Zr, Si, Hf).

Those various metallic fuels in combination with LOX are being called LOX-pyrolant (coruscative) [4].

There are numerous advantages using the LOX-Ex technologies.

Blasting technology:

- LOX-Ex has a high energy density - about twice as much compared to TNT.
- Self-defusing of duds.
- High detonation speed which can be chosen from 1,500 m/s up to approx. 9,000 m/s and therefore high power density.
- Inexpensive LOX-Ex-pyrolant primer are being used to ignite LOX-Ex in an automated process.
- The LOX-Ex fuel in combination with the LOX-Ex-pyrolant primer are very suitable for automated processes because it is self-defusing due to the rapid evaporation of the liquid oxygen

- The residual fuel is not explosive nor toxic and can be recycled or is disposed together with other waste. LOX-Ex can be used in small portions. Therefore, the LOX-Ex technologies can be embedded and integrated in existing processes and manufacturing facilities.
- Comparable to similar production technologies the LOX-Ex technologies does not require large and energy consuming tools, such as sintering presses.
- A new field for the application of the LOX-Ex technologies is the recycling of granulated electronic scrap. Almost all precious metals and rare earths can be extracted from this incineration.

Safety and handling:

- The fuel of LOX-Ex is not explosive. Therefore the fuel can be transported through public places and stored at public places without any special safety considerations.
- LOX-Ex is generated at it's location of usage. LOX-Ex can be stored in dewar containers.
- The fuel, LOX and the pyrolant primer are not subject to laws concerning explosives, therefore no book keeping is required.
- It is possible to re-drill a blasted borehole instantly, because LOX is evaporating rapidly.
- The swaths are free of nitrogen oxides.

Financial considerations

- LOX-Ex is very cost efficient, depending on the fuel and the amount used as low as 0.50 €/kg.
- LOX-Ex can be designed with target specific properties.
- Since none of the fuels are explosives no otherwise necessary and very costly safety precautions and considerations have to be made in order to transport or to store the fuel.
- LOX-Ex has about twice the rock-breaking effect as ANFO. The drilling effort in reference to the diameter can be reduced by 50%. Since PMMA-LOX-Ex has a higher density compared to ANFO the diameter of a borehole could be even reduced to 1/3.

1.2. Comparison of LOX-Ex to other explosives

Most available explosives are one component materials where oxygen is in a chemical binding. A part of the total energy is being used to free the oxygen, which reduces the energy available for the detonation. The LOX-Ex technologies use a mixture out of a fuel in form of open molecular structured nano-particles of a specific chemical substance and liquid oxygen. This guaranties a high energy density and a detonation speed of up to 9000 m/s. Still, such mixtures are safe to handle and require an ignitor [1].

Table 1 compares various explosives in reference to density, explosive heat, and detonation speed.

Explosive	Density g/cm³	Explosive heat * kJ/kg	Detonation speed m/s
Blackpowder	1,1	2784	400
Nitroglycerin	1,6	6238	7600
Glycoldinitrat	1,49	6615	7300
Nitrocellulose	1,67	4396	6800
Nitropenta	1,77	5862	8400
TNT	1,65	3977	6900
Hexogen	1,82	5277	8750
Octogen	1,89	5680	9110
ANFO	0,8	3700	3000
PMMA-LOX-Ex	1,142	8980	7000-9000
PS-PMMA-LOX-Ex	1,102	9761	approx 7000
PP-PMMA-LOX-Ex	1,071	9817	approx 7000

Tabel 1 *values depend on the method of calculation.

2. The principle of handling of the explosives in the LOX-Ex technologies

2.1. General handling

Using the LOX-Ex technologies is a very easily to handle process. The fuel and the ignitor substances are being stored separately in a dry environment.
The INBT tested several methods within different projects for mining and tunnelling successfully (compare with 3. Examples for automation in mining and tunnelling) with an automated LOX-Ex mixing, portioning, and firing procedure. The steps for the manual or the automated procedure are:

- Delivering of the fuels, ignitors, LOX and capsules for the LOX-Ex mixture from the storage.
- Pre-cooling of the fuel (brief storage of the fuel in a cooled environment).
- Portioning of the fuel, LOX, and mixing to LOX-Ex.
- Filling of the capsules.
- Firing of the capsules with the LOX-Ex charge.

Picture 1 and 2 show a fuel pre-cooler (volume 25 liter) and a dewar storage container (volume 10 liter). It is possible to use regular thermos container out of stainless steel for smaller amounts. To allow self-cooling by evaporation all containers must not be hermetically closed.

Pic. 1: Fuel pre-cooler

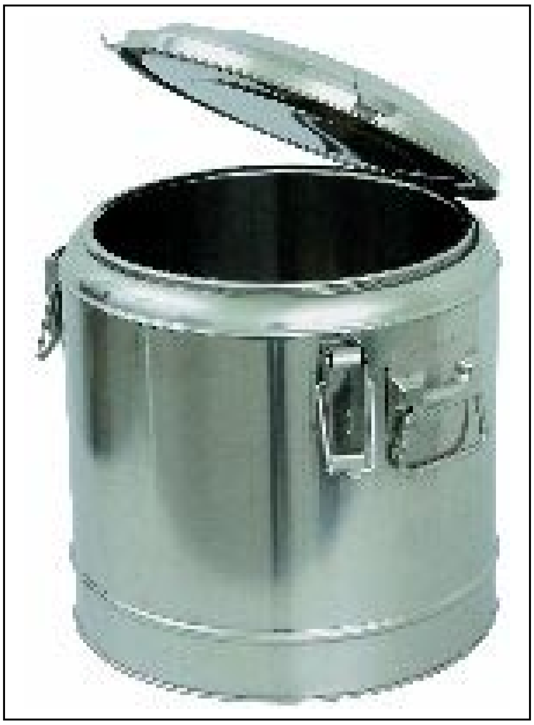

Pic. 2: Storage dewar container for the LOX-Ex

2.2. Specific handling

2.2.1. Continuous shooting

Picture 3 a, b and c show an automate for the filling of the capsules with PMMA-LOX-Ex. This automate is a part of the in "3. Example for automation in mining and tunnelling" featured continuous shooting apparatus.

This machine fills the empty pre-cooled capsules with LOX-Ex and moves the charged capsules to the transvector (pneumatic ring jet nozzle). The capsule is ready to be fired.

Picture 3 a - c: View of the rotary conveyor of the LOX-Ex filling machine

2.2.2. To create intermetallic compounds

With LOX-Ex technologies it was worldwide to the first time possible to create intermetallic of otherwise inert metals, such as tungsten carbide or Stellite® with stainless steel.

The INBT conducted a series of experiments to create individually various intermetallic compounds; examples are listed under point 4.

Because of the uniqueness all the steps of preparation and firing where done manually. However, to create a series of the same product it is possible to automate the process. Picture 4 a - c show

a) a pre-fabricated form out of styrofoam, which contains the metal parts and the LOX-Ex.

b) The styrofoam form with the ignitor is on top of a sturdy baseplate or foundation.

c) Successful detonation.

Pic. 4 a, b and c: Process to create intermetallic compounds

Unused LOX-Ex is being disarmed by evaporation of the LOX. The fuel, in this case PMMA, is disposed or could be reused (pic. 5).

Pic. 5: Disposal of PMMA-LOX-Ex; here approx. 300 g

3. Examples for automation in mining and tunnelling

Many steps of the process in mining and tunnelling are partially or fully automated. However, the application of traditional explosives creates the problem of duds. It is difficult to check the success of a detonation. Residual explosives and duds make it dangerous to re-drill or to remove the overburden. The nature of conventional explosives makes it impossible to utilise continuous applications. LOX-Ex has a high brisance and can be used in high clock frequency and it is, compared to other explosives with a similar high brisance, inexpensive.

3.1 The LOX-Ex-Method

The INBT developed a LOX-Ex technology for the automation of mining and tunnelling. Common is in all ways the automated mixing of the explosives and the filling of the capsules to fire them pneumatically at different rock-formations. The explosion is triggered due to the impact at the surface of the rock – LOX-pyrolant ignites the charged capsule.
The pyrolant igniter is inexpensive and without LOX absolutely inert. It is possible to realise this LOX-Ex technology in various ways, pictured in 6 a-c.

a) frontal fire at a wall with compact or/and shape charges,
b) shoot at a borehole (here is the charge diameter larger than the borehole diameter)
c) shoot into a borehole.

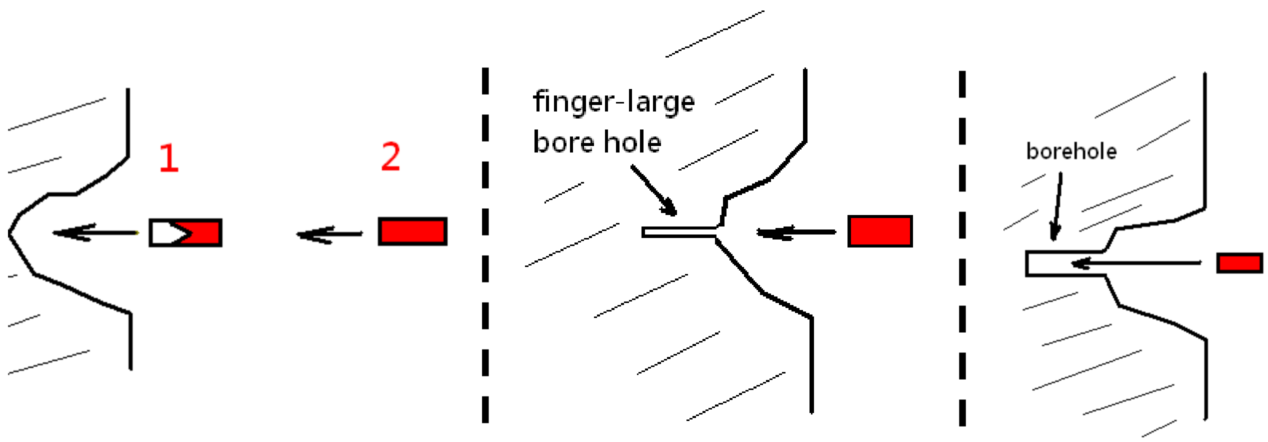

Pic. 6 a, b, c

Here a link to test of the automated shooting system according to the variant of the picture 6 a) https://www.youtube.com/watch?v=lWUI0cLXRtw

This LOX-Ex-technology is based on the method of drilling and blasting by Loui [5] and the AAI Corporation [6] to [10].
Loui and the AAI Cooperation used C4 explosive. However, usage of C4 is not approved for the civilian sector.

Picture 7 a and b demonstrate the positioning of the prototype of the LOX-Ex technology machine for continuous shooting in front of a wall of anhydrid.
The transvector and the filling automate are clearly visible in picture 7 a.
The shooting apparatus is a pneumatic transvector with a concentric ring jet nozzle. The charged capsules are accelerated to reach a velocity of up to 50 m/s towards the wall.
Picture 7 b shows successful rock-erosion by LOX-Ex shooting. Details and graphics can be researched in [3].

Pic. 7 a, b: The LOX-Ex method in action

Here is a video for this test; frontal fire on rock wall:
https://www.youtube.com/watch?v=o87CshXBc60

Picture 8 shows a batch of prepared plastic capsules with a LOX-pyrolant ignitor ready to be filled with the mix of fuel and LOX

Pic. 8: Prepared plastic capsules

All three methods (pic. 6) of shooting explosives were tested with the equipment seen in pictures 7. The results are summarized and evaluated in [3].

The INBT also conducted a simulation to clean furnaces of thermal power plants with the LOX-Ex technology using very small charges.

Smaller side galleries are being excavated from an accessible and passable main gallery in the pattern of a herringbone structure in order to extract the less productive layers with automated equipment.
Such mines could be exploited much longer and still being profitable.

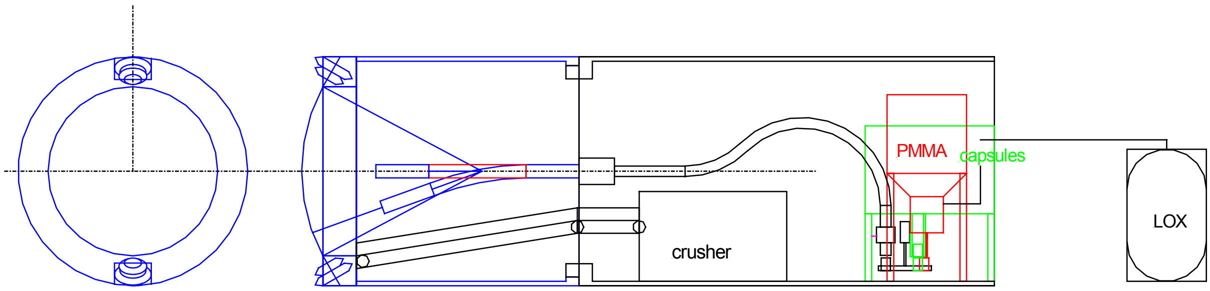

Pic. 9: Modules of the LOX-Ex method integrated in tunnel boring machine

All three methods tested can be applied in a tunnelling unit which includes the LOX-Ex machine (pic. 9) together with other traditional mining and tunnelling equipment, such as conveyor belts to remove excavation material, construction and other supporting equipment.

This LOX-Ex technology can be used within the subterranean ore mining in a continuous process where the thickness of the layer of ore containing material became to little to use traditional extracting methods and equipment.

The combination of continuous, alternating drilling and shooting is highly effective, excavated materials are being removed on conveyor belts or with other suitable equipment.

Another technology invented, created, and successfully tested by the INBT is the application of a "blasting star". This technology was presented to the first time at the 19. "BSK" (mining and blasting technologies colloquium) at the University Clausthal-Cellerfeld, Institute of Mining [11]. The "blasting star" technology is based on the principle of explosive cutting charges [12].
The "blasting star" technology uses rotational symmetric placed cutting charges.

A “blasting star” of any desired length is being placed in a matching bore-hole. The explosion causes a radial limited destruction of the rock-formation around the bore-hole. In other words the bore-hole is widened radial to a significant larger tunnel. A well adapted “blasting star” reduces damages to neighbouring rock-formations.
A “blasting star” could be applied together with the LOX-Ex technology in less productive ore mines as described previously. The lining material in this case is barite embedded in cement instead of copper.

It is important for the subterranean mining to keep disturbances of the rock-formations at a minimum. Therefore, low impact charges have to be applied. The LOX-Ex technology offers the advantage of small charges with a maximum effect. Excavated materials and waste products, such as H_2O and CO_2, can be continuously removed without facing the danger of duds and residual explosives.

3.2. Spiral Explosive Boring/Mining with Mini-LOX-Ex-Loads

The INBT tested a spiral explosive boring/mining process with very small explosive charges by manually simulating the automated process.
With the LOX-Ex technologies it is possible to operate the process remotely and automatically, while the shooting angle can be adapted immediately to the technical requirements.
Again, because of small charges the process is very safe for man and machines.
Picture 10 a and b illustrate the principle of spiral explosive boring/mining. The process was repeated with changing shooting angles.
Picture 11 shows the experimental results of a drilling with single-loads of 25 g PMMA-LOX-Ex.

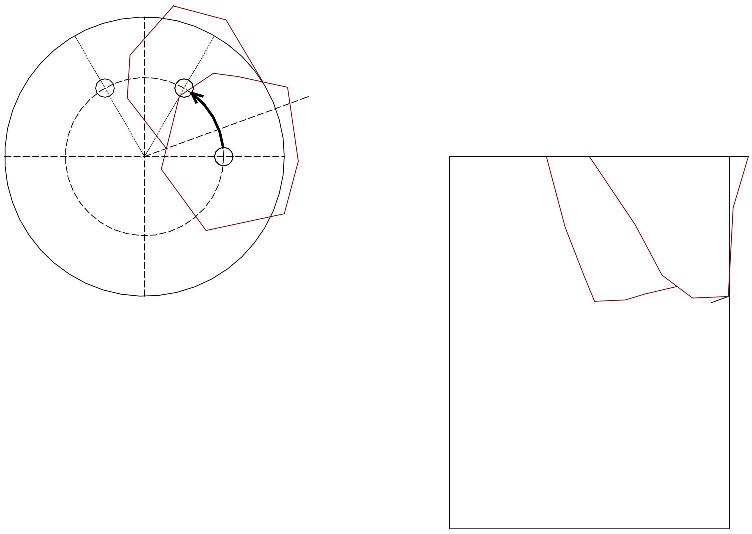

Pic. 10 a) Top view   10 b) Cross cutcut

In these tests the loads were ignited with standard electrical detonator, which worked perfectly even at low temperatures of liquid oxygen. Table 2 shows the test results of seven consecutive explosions, each 25 g PMMA-LOX-Ex. As a result a hole with a depth of 51 cm was excavated and 100 liter anhydrid were removed.

The optimal height of layers removed is between 100 cm and 150 cm. Each PMMA-LOX-Ex charge does not exceed 150 g. Such a machine can reach a production volume performance between 30 m³ and 50 m³ per hour.

Charge Nr.	Angle °	Depth cm	Length cm	Width cm	Excavitation liter
1	0	16			
2	60	23			
3	120	24	80	80	38
4	270	27	80	90	49
5	360	33	90	90	67
6	450	35			
7	600	51	90	100	97

Tab. 2

Another way is to pneumatically shoot an explosive capsule into the bore hole.
Thirdly it is also possible to use the special developed pneumatic pyrolant-ignition for fixed loads. This ignition does not need an ignition capsule with an additional explosive. The capsule is filled with an metallic pyrolant only.
Since the capsule does not contain LOX it is safe to handle, to transport and to store, and the administrative effort is nearly zero.

The tested spiral explosive boring/mining process can be utilised in quarries. Special blasting machines will work remotely controlled and automated. The target area is covered and shielded by the front part of the blasting-machine to reduce noise and to direct loose materials onto conveyor belts.

4. LOX-Ex for automated Production Technology Material Processing and Syntheses

Explosives are used for production technologies in material processing since about 50 years. Since today following processes are established:

- Cutting and perforating
- Forming
- Welding
- Compacting metal powders
- Cladding of metal layer
- Hardening
- Syntheses of hard materials (e.g. micro-diamonds)

With the LOX-Ex technology it is easy to embed workplaces with explosives using for material processing in production processes - also retrospectively in already existing systems.
Picture 11 shows the scheme of an automated LOX-Ex using production facility. The stations 1 to 5 indicate possible preparation places for the LOX Ex application, the workpiece is automated and remotely controlled moved to station 6 (explosion location).

Such a facility would be suitable for the production of a polycrystalline diamonds. The INBT tested in experiments the possibility to use up to 300 g PMMA-LOX-Ex.

In case the automatic production process stops unexpectedly, LOX evaporates immediately and the production facility secures itself.

Station 6 could contain an arrangement like it was used in tests shown in pic. 4 to produce new intermetallic compounds. The following scheme 12 demonstrates a filled and for ignition prepared explosion arrangement.

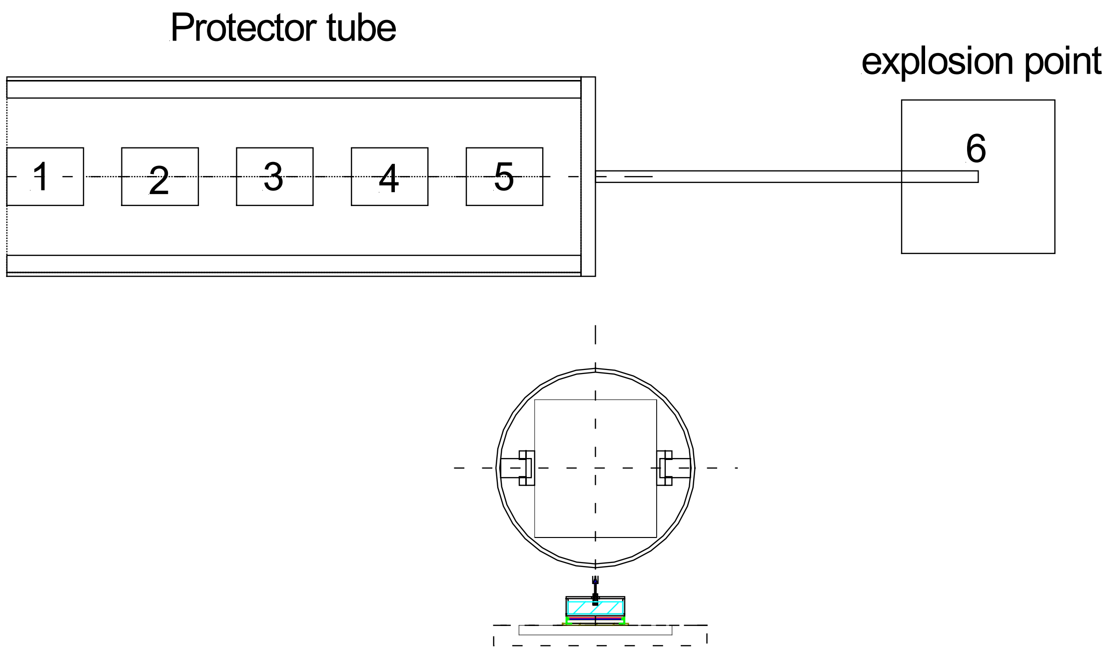

Pic. 11: Scheme of an automated explosion production facility with LOX-Ex

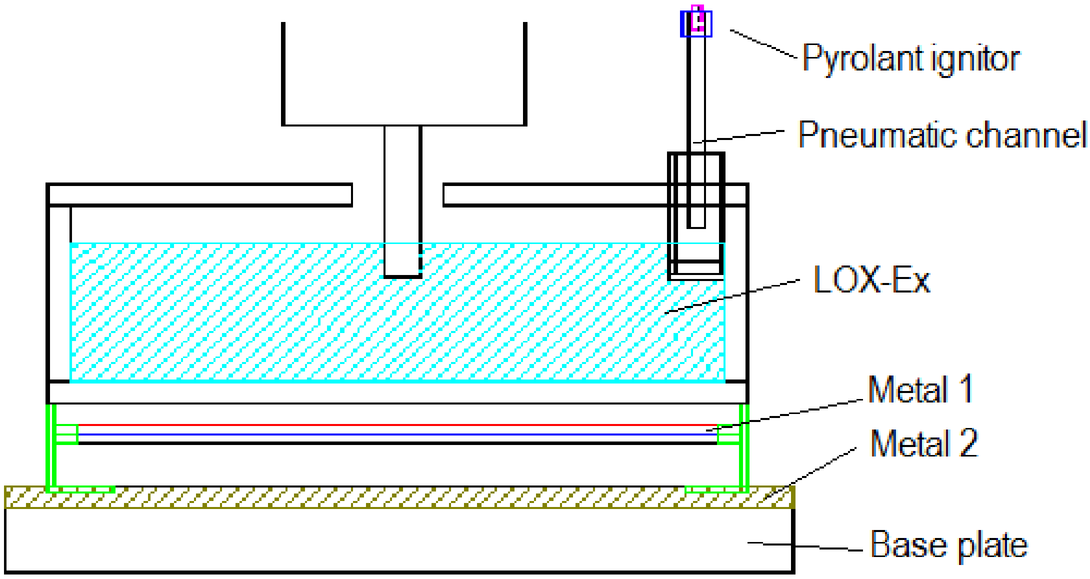

Pic. 12: Example of a filled explosion arrangement

Right on top is the pyrolant ignitor-impact.
The pneumatically driven pyrolant ignitor-impact was developed and tested at stationary loads by the INBT in 2013. It should be noted, that the pyrolant ignitor-impact was also used in experiments described in point "3.1. The LOX-Ex-Method".

4.1. Special prospects for LOX-Ex: Automated material forming processes

Explosives were used in an automated production process in th e automotive industry of the GDR. During the seventies of last century East Germany produced in an automated series production metal parts applying small explosive charges for certain process step
[13].

In the US, parts of the rocket nozzle of the Saturn 5 rocket were formed by the use of explosives.

Because these processes require a great deal of work and security, they are no longer used as often. With such masses industry area must lay in a great distance to explosion application.

The properties of LOX-Ex make it possible to revive the series production of formed parts with explosives and make it profitable.

4.2. Using of LOX-Ex on the field of material synthesis

In the past unsuccessful attempts have been made to combine tungsten carbide and steel intermetallically.
The INBT succeeded in producing a workpiece made out off tungsten carbide and steel (stainless and construction steel), picture 13, in an intermetallic combination using LOX-Ex technologies.

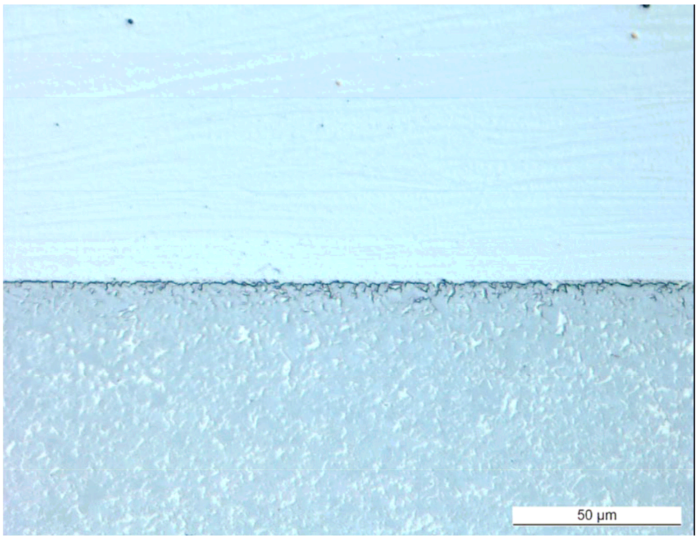

Pic. 13: Bonding surface between mild steel S235 and tungsten carbide hard metal

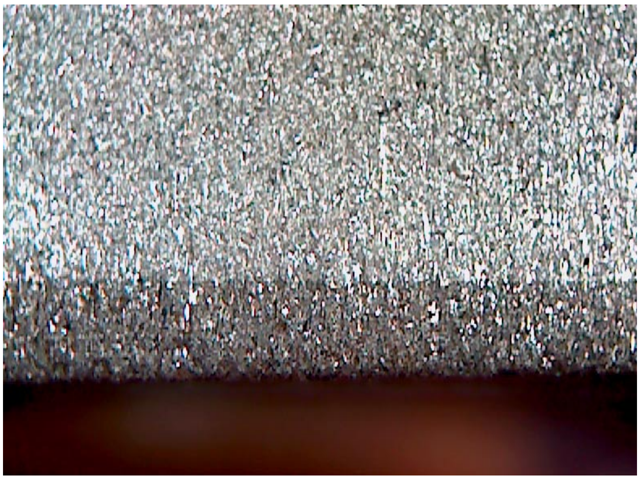

Pic. 14: Bonding between INCONEL and niobium

According to the experimental setup, which can be seen in Figure 4 and is shown schematically in Picture 12, it was also possible to establish a connection between INCONELL and niobium, pic 14, and between steel and STELLITE.

Two- and three-layer material samples were produced. Picture 15 shows a triple layer;

The proof of the successful connection was provided by the ISAF Institute of Welding and Machining, TU Clausthal [14].

Pic. 15: Triple layer; below steel; mid titanium; on top copper

In other experiments, both steel and copper were combined with tungsten carbide powder by the use of LOX-Ex.

Picture 16 shows an example in which was blown up STELLITE granules on steel (usable for wear protection).

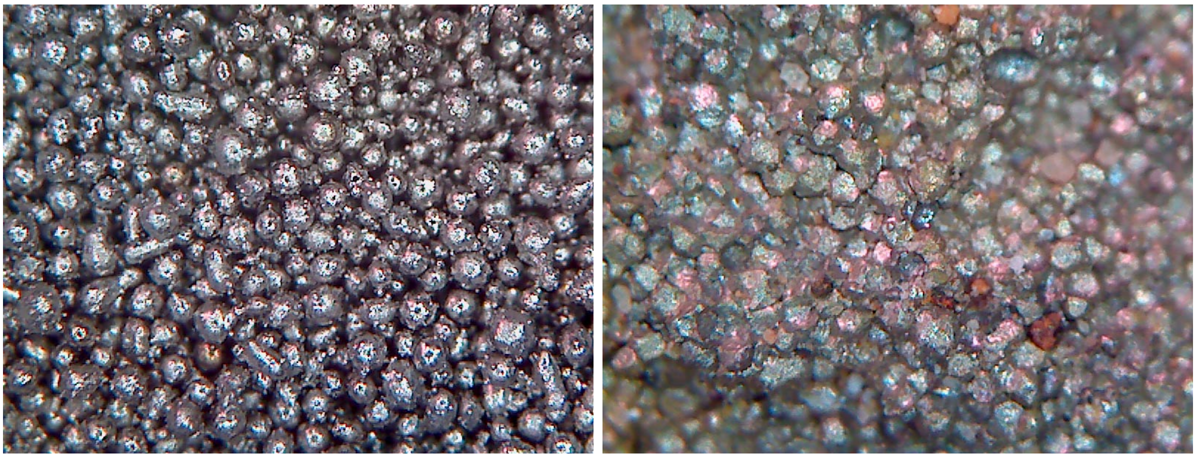

Pic. 16: Stellite granules on steel; left before, right after explosion

Additonally defined pieces of tungsten carbide bits were implanted in steel. Those tungsten carbide bits kept there shape and didn't show any sign of breakage. This is an application in the production of drill heads.

Although each of these experiments has been manually prepared and performed, it is possible to automate the process.
The advantages of the LOX-EX technology (low cost, high safety in handling, no accounting, etc.) make the application very profitable.

5. Conclusion

The INBT developed a new class of explosives called LOX-Ex (Liquid Oxygen Explosives). The explosive consists of two components, the molecular structured nanoparticles of a substance as fuel and liquid oxygen as oxidant.

With the availability of these newly developed and successfully tested liquid oxygen explosives and the associated new LOX-Ex technologies, numerous blasting processes in the areas of mining, transport infrastructure (tunnelling), material processing and material can be partially or fully automated.

LOX-Ex technologies can be used to dig tunnels faster, extract resources more efficiently, and exploit inefficient resource deposits.
LOX-Ex technologies can find application in the molding of components.
LOX-Ex technologies have been successfully tested in the creation of new materials.
Automated LOX-EX technologies can be used in areas that are dangerous to people, difficult to access, or inaccessible.

It is conceivable that an "ore-drone" will be used as an autonomous working mining machine.

Instead of using large quantities of conventional explosives at once, automated LOX-Ex technologies offer the advantage of using small amounts of explosives in high frequency and continuously. This means less noise, less vibration and a lower need for ventilation because there are no nitrogen oxides. LOX-Ex technologies can be easily integrated into existing automated processes.
Neither LOX-Ex nor its components have explosive properties. LOX-Ex ensures more safety in storage and application. LOX-Ex is environmentally friendly. The reaction products of PMMA-, PP- , and PS-LOX-Ex are only H_2O and CO_2
LOX-Explosives are self deactivating LOX-Ex reduces the bureaucracy. Pyrolant-igniters are inexpensive, not explosive and do not require book keeping.

Mr. Dr. Claus Becker
LOX-Ex technologies

Acknowledgements:

We appreciate the help and support of:
- KNAUF Deutsche Gipswerke KG, Rottleberode
- BAUER Maschinen GmbH, Schrobenhausen
- Schmidt, Kranz & Co. GmbH
- Prof. Th. M. Klapötke, Ludwig-Maximilian University, Munich
- HAZEMAG EPR GmbH
- Starck GmbH
- BETEK GmbH
- ISAF, TU Clausthal-Zellerfeld
- BAM, Berlin
- KANEKA (Japan)

Special thanks to Mr. Roland Menzel for his support with the translation of the text.


BLASTANE
High purity hydrocarbon fluids for Ammonium Nitrate explosives
BLASTING RESPONSIBLY
www.totalspecialfluids.com
TOTAL
Committed to Better Energy

Borehole Deviation Control Using Electronics: An Euler's Approach

Abstract

The consequences of rock blasting with explosives are directly related to the accuracy of drilling and, because they have an effect on fragmentation and ground level, they should be controlled to ensure a problem free production, increase work safety and reduce environment impact. Safety control is one of the most important processes in detonation, since it can compromise the worker security on site and, eventually, neighboring communities. Due to the technology advancements, it is possible to build a hole deviation control device with "of the shelf" parts, and for that reason the authors decided to evaluate the possibility of measuring hole deviation by creating a portable prototype using an electronic sensor capable of measuring the acceleration on objects, that is, to measure the own acceleration of a system, known as "accelerometer" and a micro-controller to handle and treat data. The main idea behind this paper is to validate the power of the Euler method, given the stepping limitations of the sensor and micro controller in order to reproduce of the hole shape. A case study was carried out, comparing the measurements of borehole deviations made by a traditional equipment and the prototype.

A mobile application was also created in order to recover and treat and display the data to the user. For validation of the prototype, several holes were measured using the two devices. A residue analysis was used to validate the data obtained. After analyzing and confirming the effectiveness of the new equipment, the normality tests prove a symmetric distribution with null expected residual mean and minimum variance. Consequently, the accuracy of the prototype is evidenced. Thus, the authors aspire to emphasize the potential of using these sensors allied to a traditional numerical method for analysis of hole deviation.

Introduction

Rock blasting aims to divide a certain amount of rock mass into smaller pieces (at the lowest cost possible). This procedure is applied in the majority of mining operations, quarries, civil engineering applications and even in some cases of ornamental rock operations. Therefore, the conditions that the rock blasting process is carried out affects directly the operation´s results (Bhandari, 1997). For this, the precision in the steps of rock blasting to achieve the planned objectives and the knowledge of the rock conditions are essential in order to obtain the desired fragmentation (López Jimeno, López Jimeno, & Garcia Bermudes, 2017).

Drilling is one of the most important steps in this process. Consequently, the control and the prior knowledge of drilling results is essential to proceed with the planned blast, maintaining the necessary economy throughout the cycle of mining operations (Leite, Miranda, & Palangio, 2018). It is called a drilling deviation when a hole is subjected to an unintended abnormality of a planned trajectory. The deviation of the path of the planned hole can lead to problems such as high cost of drilling, fragmentation issues, fly rocks, irregularities in the floor or ramps, damages to the instrument, among others (Harris, 1999). In addition, the analysis of the profile of the borehole with the use of deviation measurement equipment allows the control and minimization of toe generation, over excavation, slope stability and monitoring of drilling operations (Miranda & Leite, 2018).

Figure 1. O-PitDev Developed System

The focus of this project was the research and creation of a prototype of a hole deviation measurement equipment, named as *O-PitDev.* The main idea behind this work was to validate the power of the Euler method, given the size of the pitch generated by the sensors used in the equipment, for the reproduction of the hole shape. A case study was conducted comparing the results of hole-deviation measurements performed by traditional equipment compared to the developed one, communicating it with *O-Pitblast* installed in a mobile application to manage the equipment. For the validation of the prototype, the measurement of several holes was taken through the 2 (two) methodologies. A residue analysis was used to validate the data obtained and after the analysis, the effectiveness of this tool was confirmed, considering that the normality tests proved a symmetrical distribution with zero residual mean and minimum variance. Thus, the researchers proved throughout this article the potential of the use of these sensors allied to a traditional numerical method for the analysis of deviations of holes.

Deviation issues

For many rock blast operations there is the need to protect the surround environment. Drill deviation can originate vibrations, noise, fly-rock and other problems that can be avoided with caution blast procedures and blast analysis.

Production issues

Larger blocks that require secondary blast or excess fines may result from poorly designed shots or from adverse geological conditions. Damage to the hanging walls and dilution are other examples of production issues caused by irregular drilling. The same in over break caused by imprecise drilling (Bhandari, 1997).

Deviated holes can lead to bad fragmentation, due to the increment on burden and spacing along the borehole from the collar to the bottom. To one hole near the crest, if the inclination is higher than the plan a higher concentration on powder factor will be generated near it– condition that can reduce the efficiency on the borehole bottom and the production of toes. In the other side if the subdrill is smaller due to drill errors, the probability for toe generation will increase along with the cost for drilling, load and haul (López Jimeno, López Jimeno, & Garcia Bermudes, 2017).

Safety issues

Non-controlled blast can compromise the viability of a project, whether due to community complains, damage to adjacent structures resulting in legal problem and putting live at risks. Drilling error (low subdrilll, excess subdrill, hole very close to a free face) can lead to bad fragmentation followed by ground movement, vibrations, air blast, toxic gases and fly rocks.

Deviation measurements

The need to control your blasts' results is always increasing and, having that in mind, the mining companies are continuously seeking for ways to improve and predict outcomes. The measurement of a borehole deviation is an important step to that market, that's why the companies are always evolving and introducing new devices to the market. In this chapter the authors will give some examples of equipment that are already present in the mining world.

Measurement devices

There is a diverse number of equipment with a common objective: measurement of boreholes deviation. As an example, the market has the Boretrak from Carlson, Blasthole Probe from Pulsar and even an Android smartphone (Miranda & Leite, 2018).

Blasthole probe

This tool allows the user to see the inclination, heading, depth and presence of water of the holes. The procedure is simple: the operator lowers the probe and take measurements by an interval defined by him. This probe has a winch and a cable attached. The accuracy of this device is ± 0.25º for the inclination and ± 1º for the azimuth (Ewer, 2018).

Rodded boretrak

The Rodded Boretrak is can be used in metal operations and is composed by multiple bars that allow the operator to measure the borehole deviation meter by meter. Also, it can be used in upholes that are very common in underground mines. It has an accuracy of 0,1º and it can take inclinations until 45º (Renishaw,2017)

Cabled boretrak

This device has a different usage methodology. In this case, the device is attached to a cable that is marked meter by meter. It can't be used in metal operations and its only prepared to do downholes. It's based on a digital compass and a dual axis tilt sensor. The accuracy and maximum inclinations are the same as the rodded boretrak®: 0,1º and 45º, respectively (Renishaw, 2017).

Figure 2. Rodded Boretrak (left) and Cable Boretrak (right)

Android smartphone

This new technology based on a smartphone, that was presented by in Fragblast 12' (Miranda & Leite, The use of 3D accelerometers and gyro sensors in smartphones to measure the blasthole deviation in non- magnetic rock, 2018), it's apparently less complex, easy to use and cheaper. The research uses the accelerometer and the magnetic sensor present in the Samsung Galaxy S8 to make the measurement of the hole deviation. The operating mode is based in two apps where the operator puts the offset and the range, in meters, that he wants to make the measurements. In the end, the data from both phones is combined and the result is a file that contains the borehole data: number, inclination and time of measuring.

Figure 3. Smartphone used to measure holes

Measurement results

After the field procedure, either with smartphone technology or any other device with the same propose, the operator gets the information of the real inclination, heading and depth of the borehole. With that information and with a blast design software, it's possible to analyze different situations/problems such as:

- Critical profiles: rows too near/far from the free face;
- Critical burden;
- Projection risks: hole not drilled correctly (their inclination/azimuth is wrong) causing fly rock risks;

- Burden distribution;
- Deviation values; y
- Real angle: possibility to see if the planned hole and the real one has the same angle;
- Toe error: generation of toe due to a wrong drilling.

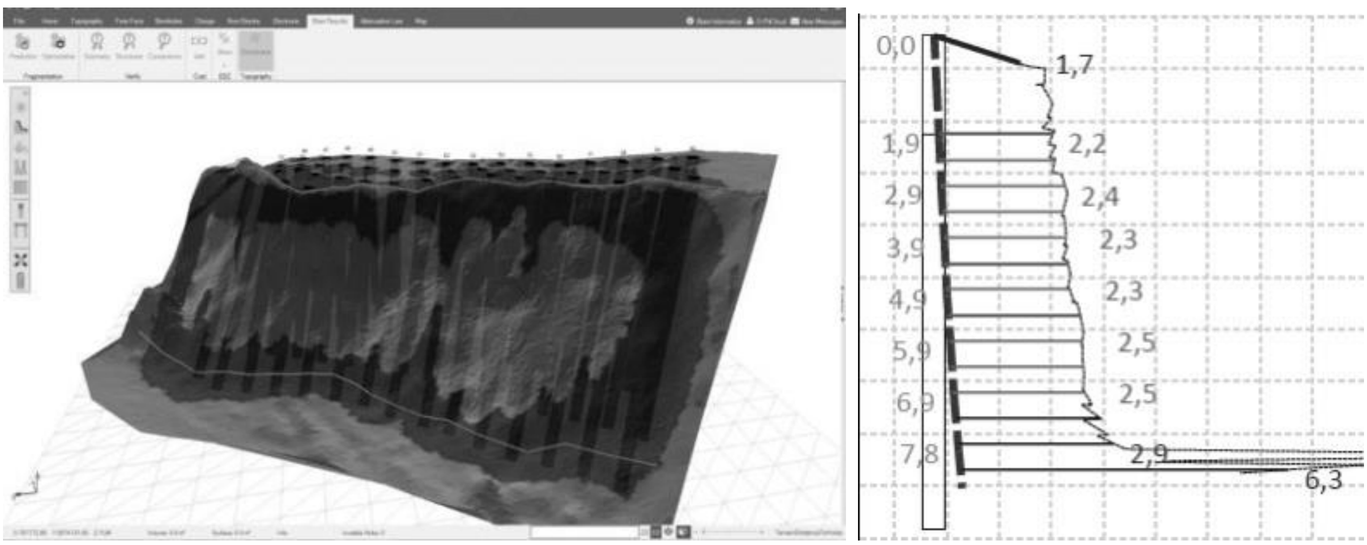

Figure 4. Critical Burden Detection (O-Pitblast)

Euler Method

In order to fix numerical problems with the format below, Euler proposed a solution based on the previously knowledge about the behavior of the function (Butcher, 2003) :

Equation .

$$y'(t) = f(t, y(t)), \quad y(t_0) = y_0$$

Starting from a known point, the next iteration is approached by the following equation:

Equation 2

$$y(t_1) \approx y_1 = y_0 + hf(t_0, y_0)$$

Where h is the size of the step used for each measurement.

The image Figure 5 shows the real solution for a generic example and the Euler's approach for different steps (10 and 100 steps) and we can observe that for highest values of step the solution is closer of the real one.

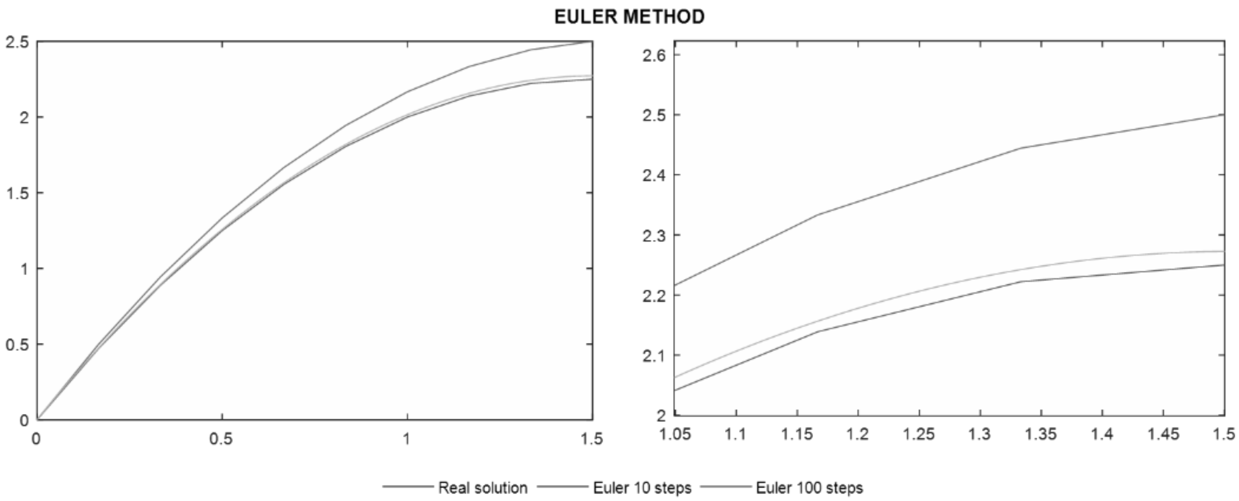

Figure 5. Euler method example

Phone app

To make it possible to observe the results on the field immediately after the measurements were taken, an Android app was developed. The Android app works with both the traditional method, (measuring angle and heading meter by meter) and with the Euler method (measuring the linear acceleration as many times as the electronics allowed). After receiving the data, the app calculates the profile of the hole and displays it to the user.

Probe Electronics

A ESP32 microcontroller was used in this research due to the fact of being power efficient, fast, and having Bluetooth capability. The micro controller was paired with the sensor BNO055 from Bosch Electronics, a 9 DOF sensor with an accelerometer, gyro and magnetometer using I2C. In the traditional approach a combination of the three sensors is used to calculate heading and inclination, on the Euler method a "sensor fusion" method called linear acceleration is used in order to eliminate gravity from the results.

An internal memory chip of 4MB was used to record all the data. According to our estimations, recording 3 different measurements (x, y, z) each millisecond, would allow us space for only 5 minutes of measurements.

Connection

Bluetooth was the choice of communication between the probe and the phone due to the high availability (a large portion of smartphones have it) and there is a Bluetooth module present in the ESP32 microcontroller we referenced earlier. The communication is not real-time since when the probe is inserted into the hole, the signal is lost. Internal memory is used while the probe is inside the hole. The data is transferred back to the phone as soon as the probe reconnects to it.

Probe Case

To introduce the sensors and electronics so that they remain intact and running through a hole, an AISI 304 stainless steel cap was designed. In the planning of the capsule, it was investigated that stainless steel does not isolate the radiofrequency necessary to communicate the data between the equipment and the receivers installed in PC and in mobile phone, thus dispensing with the installation of an external antenna for connectivity between both. In addition, the choice of stainless steel was due to its famous resistance to corrosion, giving a longer life than other materials and elements. But despite being the main feature, there are several other advantages of using stainless steel (Frank, 2009) such as:

corrosion, giving a longer life than other materials and elements. But despite being the main feature, there are several other advantages of using stainless steel (Frank, 2009) such as:

- Physical (mechanical) resistance equal to or greater than ordinary steel;
- Ease of cleaning;
- Low surface tension;
- Hygienic appearance;
- Inert material (does not react to contact with other materials);
- High durability and shelf life
- Ease of modulation and welding;
- Stability in extreme temperatures;
- Visual beauty (modernity, cleanliness and brightness);
- Great cost benefit;
- Recyclable material.

The steel case was design on AutoDesk Inventor Professional and resisted the water present in some holes, the impact on the descent to the bottom of the hole, and the friction with the wall of the hole due to the hoisting of the equipment. It has enough weight and density to overcome the thrust with fluids present in the holes, because a casing made essentially of stainless steel, material of considerable density (7.85 g / cm3) was used (Solução completa em Usinagem, 2018).

The initial idea of this first equipment was to test in the laboratory and in the field the electronic components and its connectivity and system of acquisition of data and radiofrequency transmission. The prototype cable connected to the capsule was marked every meter to set the interval for the measurements.

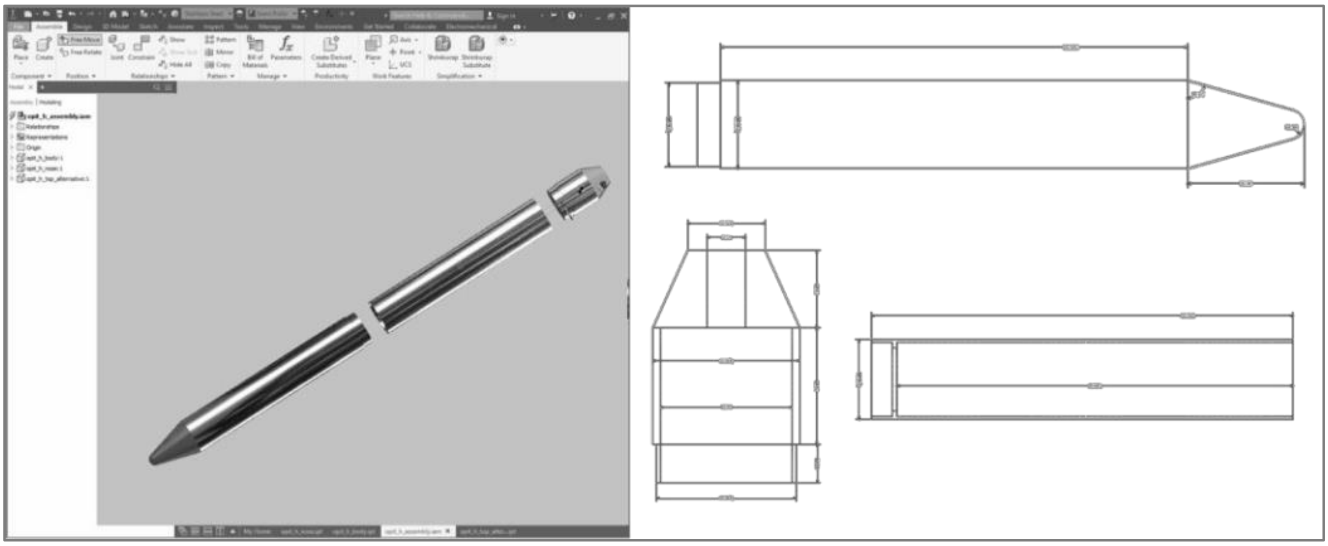

Figure 6. Case Design

Field Procedure

The field test was carried out in Madalena quarry (Vila Nova de Gaia – Portugal) explored by Solusel, Lda. The field tests included:

- Scan of the free face with Drone;
- Registration of holes position;
- Measurement of hole's profile with a Cabled Boretrak;
- Measurement of hole's profile with the developed methodology Figure 7;
  - Deployment of the *O-PitDev* in the bottom of the borehole;
  - Measurement of the offset;
  - Record the first time of the first measure in the bottom of the hole;
  - Pull the probe until the borehole collar making stops at each meter - 3.2 ft - and collect the time at those stops;
  - Match both information from phone app and probe – time, angle and azimuth.

Figure 7. Field Procedure from left to right: probe assembling; probe deployment; offset measurement; measurement time record

Data analyses

Multiple measures were recorded, inside of the borehole, at different positions. Before lowering the equipment into the borehole is define the measure interval – 1 measure at each meter (3.2 ft). In case of the hole having a size that is not multiple of the interval, the difference between the position of the first measurement and the remaining will be different. This difference is usually called off-set, while the other measures will have a difference that is equal to the interval adopted (Miranda & Leite, 2018).

Results

The researchers found some restrictions (at least with the this first approach) using the Euler's methodology due to the limitations of the sample rate Figure 8. It was possible to get around 300 samples/second which is low number when trying to obtain displacement from acceleration (applying the Euler method 2 times).

Visually the results are quite similar as observed on Figure 9. (using the inclination and heading at each meter).

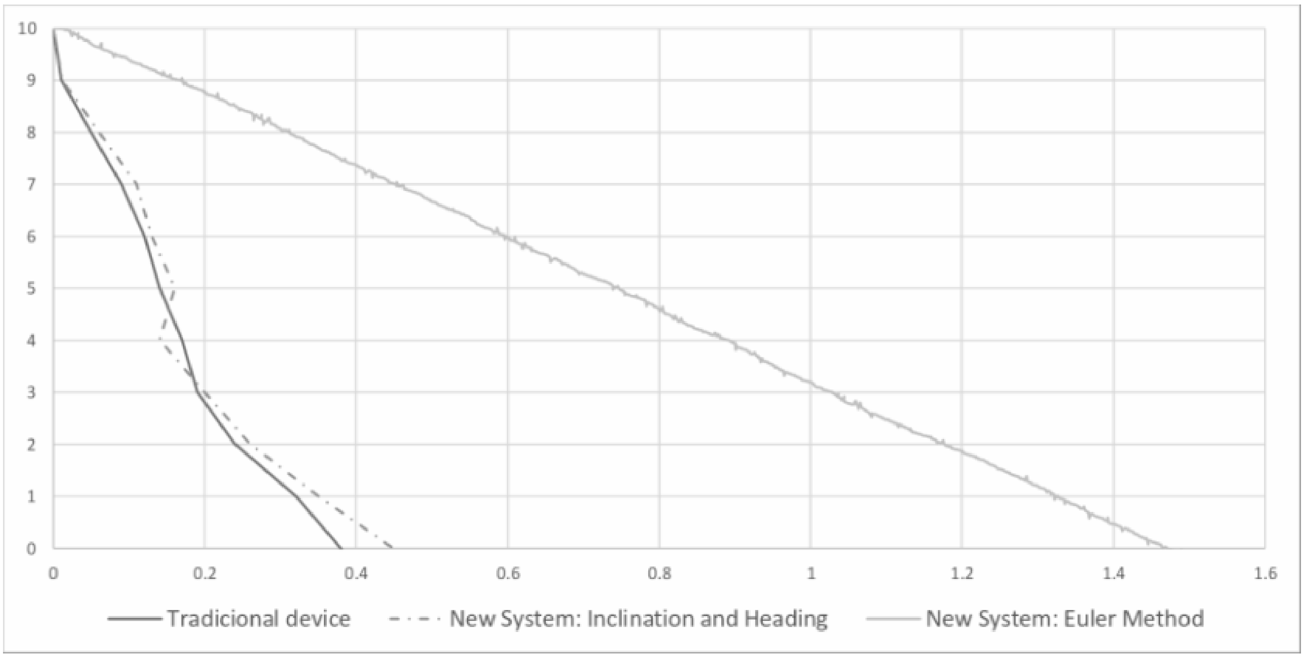

Figure 8. Comparison between Euler's methodology, heading and inclination

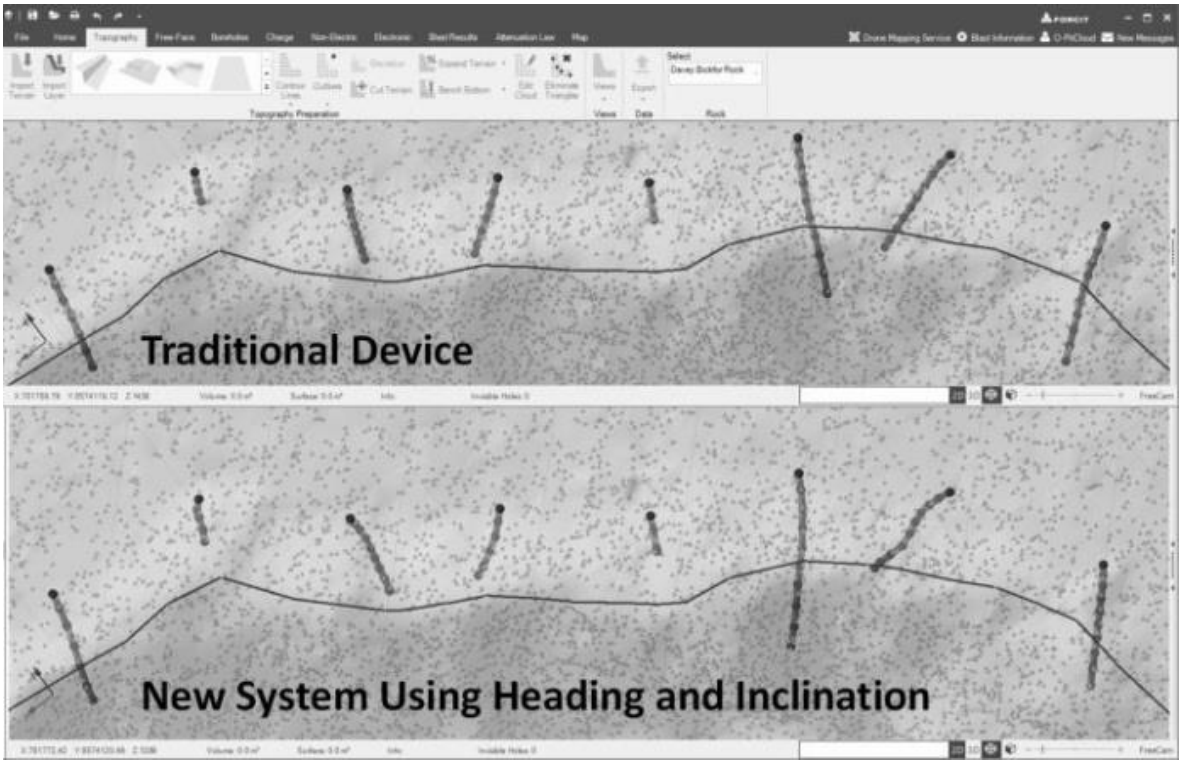

Figure 9. Comparison of devices using heading and inclination

Statistical analysis

Analyzing the residue between both data (measure with actual system and the developed one), using inclination and heading, the data shows that the new system results are equivalent to the traditional one:

- P-Value shows the acceptance of the null hypothesis (Shapiro-Wilk with 95% of confidence level)
- Figure 10 meaning that the data follows a normal distribution;
- The zero is contained within the confidence interval.

Limitations

Besides the excellent results presented by this research the authors decided to outline a couple of limitations associated with this product. This product was developed to be used only in non-metallic mines due to the effect on the magnet sensor. Some adjustments must be done on the case and the electronic system to improve a better user experience – (decrease probe weight, app design and connectivity).

Descriptives

			Statistic	Std. Error
Residue	Mean		-,0147	,00727
	95% Confidence Interval for Mean	Lower Bound	-,0309	
		Upper Bound	,0015	
	5% Trimmed Mean		-,0141	
	Median		-,0100	
	Variance		,001	
	Std. Deviation		,02412	
	Minimum		-,07	
	Maximum		,03	
	Range		,10	
	Interquartile Range		,02	
	Skewness		-,678	,661
	Kurtosis		3,127	1,279

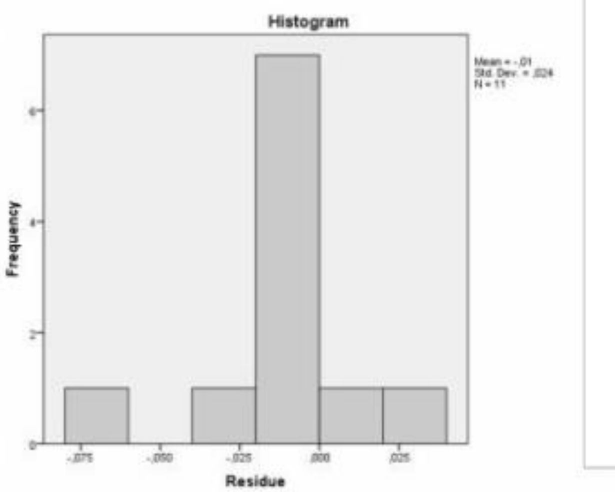

Tests of Normality

	Kolmogorov-Smirnov[a]			Shapiro-Wilk		
	Statistic	df	Sig.	Statistic	df	Sig.
Residue	,232	11	,102	,895	11	,159

a. Lilliefors Significance Correction

Figure 10. Statistics

Conclusions

Using the Euler's methodology, the authors found some restrictions about it. As mentioned on the results increasing the sample rate will be possible to obtain best results. On the research due to the limitation of the sensors used it was not possible obtain better solution. However, the results obtained using heading and inclination on the new product are extremely interesting. Be able to reproduce the obtained values with a lower cost product will definitely open new doors to small operations in order to control drill accuracy, improving safety and production.

This product allows a fast and immediate action due to the easy access to the information. The data analyzed shows a direct relation between the conventional method and the new one, proving the quality of the methodology presented. The equipment is very practical to use, the required training is low and the integration with smartphones potentializes the use of technology with the blast operation, saving time to the blast engineers.

Vinicius Miranda, O-Pitblast, Lda. and Faculdade de Engenharia da Universidade do Porto Francisco Sena Leite, O-Pitblast, Lda.

Acknowledgements

The authors would like to gratefully thank to Engineer José Guedes and Engineer João Fernandes, for the opportunity given to carry out this project in Madalena Quarry. Raquel Sobral (O-Pitblast Technical Services Engineer) is acknowledge for the outstanding support on the field procedure, patience, and excellent job on the development and quality control of the app. We would like to thank the Oporto University - Engineering Faculty (Mining Department - FEUP), specially to Engineer Alexandre Leite and Pernambuco Federal University, particularly Prof. José Carlos. A special thanks to Rosa and Carolina for the patience.

References

Bhandari, S. (1997). *Engineering Rock Blasting Operations.* Rotterdam Brookfield: A.A.Balkema. Butcher, J. C. (2003). *Numerical Methods for Ordinary Differential Equations.* New York: John Wiley & Sons.

Dowding, C. H. (1985). *Blast Vibration Monitoring and Control.* Englewood Clifs: Prentice-Hall, Inc. Ewer, M. (2018, July 7). *PULSAR MEASURING SYSTEMS LTD*. Retrieved from http://www.pulsarmeasuring.co.uk/

Frank, G. (2009). *Análise Econômica do Alumínio.* Recife, Brazil: UFPE.

Gujarati, D., & Porter, D. (2010). Econometría. México: McGraw-Hill.

Halliday, D., Resnick, R., & Walker, J. (2008). Fundamentos de Física. Volume 1. Rio de Janeiro. Hamming, R. (1973). Numerical Methods for Scientist and Engineers. New York: McGraw-Hill. Harris, J. E. (1999, Mar 12/08/2017). Drill Accuracy. ISEE: International Society of Explosives Engineers.

Hustrulid, W. (1999). *Blast Principles for Open Pit Mining.* Rotterdam Brookfield: A.A.Balkema. Instantel. (2016). Minimate Pro 6. Otawa, Ontario, Canada.

ISEE. (2015). *ISEE Field Practice Guidelines For Blasting Seismographs 2015.* Cleveland, Ohio USA: ISEE.

Jimeno, C. L., Jimeno, E. L., & Carcedo, F. J. (1995). *Drilling and Blasting of Rocks.* Rotterdam Brookfield: A.A.Balkema.

Konya, C. J., & Walter, E. J. (1990). *Surface Blast Design.* Englewood Cliffs: Prentice Hall. Lashinsky, A. (2012). *Inside Apple: How America's Most Admired--and Secretive--Company Really Works.* Business Plus; First Edition

Leite, F., Miranda, V., & Palangio, T. (2018). Pattern Expansion Optimization Model Based on Fragmentation Analysis With Drone Technology. *Proceedings of the Fourty-Four Annual Conference on Explosives and Blasting Technique.* San Antonio, Texas USA: International Society Of Explosives Engineers.

López Jimeno, C., López Jimeno, E., & Garcia Bermudes, P. (2017). *Manual de Perforación, Explosivos y Voladuras.* Madrid: ETSI Minas y Energía - Universidade Politécnica de Madrid.

Miranda, V. (2016). Validação de Modelos Lineares: Uma Análise Residual. Porto, Portugal. Miranda, V., & Leite, F. (2018). The use of 3D accelerometers and gyro sensors in smartphones to

measure the blasthole deviation in non-magnetic rock. In H. Schunnesson, & D. Johansson, *12th International Symposium on Rock Fragmentation By Blasting* (pp. 211-221). Lulea, Sweden: Lulea University of Technology, Sweden - Division of Mining and Rock Engineering.

Miranda, V., Leite, F., & Frank, G. (2017, September). Blast Pattern Expansion - A numerical Approach. *EFEE 9th World Conference.* Stockholm: EFEE.

Miranda, V., Leite, F.,Jesus, C., &

Sobral, R. (2017). A new Approach to 3D Modeling of Blast Free Faces. *International Society of Explosives Engineers - 43rd Annual Conference on Explosives & Blasting Technique - Orlando, Florida, USA*.

Miranda, V., Leite, F., Jesus, C., & Sobral, R. (2017). A New Blast Vibrations Analysis Methodology.

International Society of Explosives Engineers - 43rd Annual Conference on Explosives & Blasting Technique - Orlando, Florida, USA.

Novales Cinca, A. (1993). *Econometría.* Madrid: McGraw-Hill.

Oriard, L. L. (1999). The Effects of Vibration and Environmental Forces. *International Society of Explosives Engineers.*

Performance Specifications For Blasting Seismographs. (2016). In S. Committee. International Society of Explosives Engineers (ISEE).

Renishaw. (2017). *Rodded Boretrak and Cabled Boretrak.*

Sanchidrián, J. A., & Muñiz, E. (2000). *Curso de Tecnología de Explosivos.* Madrid: Fundación Gomez Pardo - Universidade Politécnica de Madrid (Escuela Técnica Superior de Ingenieros de Minas). Siskind, D. E. (2005). *Vibration From Blasting.* Cleveland: Internation Society of Explosives Engineers.

Solução completa em Usinagem. (2018, July 20). Retrieved from EuroAktion: http://www.euroaktion.c om.br/Tabela%20de%2 0Densidade%20dos%20 Materiais.pdf

STMicroelectronics. (n.d.). AN2960 Datasheet - STMicroelectronics. *AN2960*. http://www.st.com.

BlastMetriX UAV

Aerial 3D imaging

Blast Design and Blast Analysis with 3D images

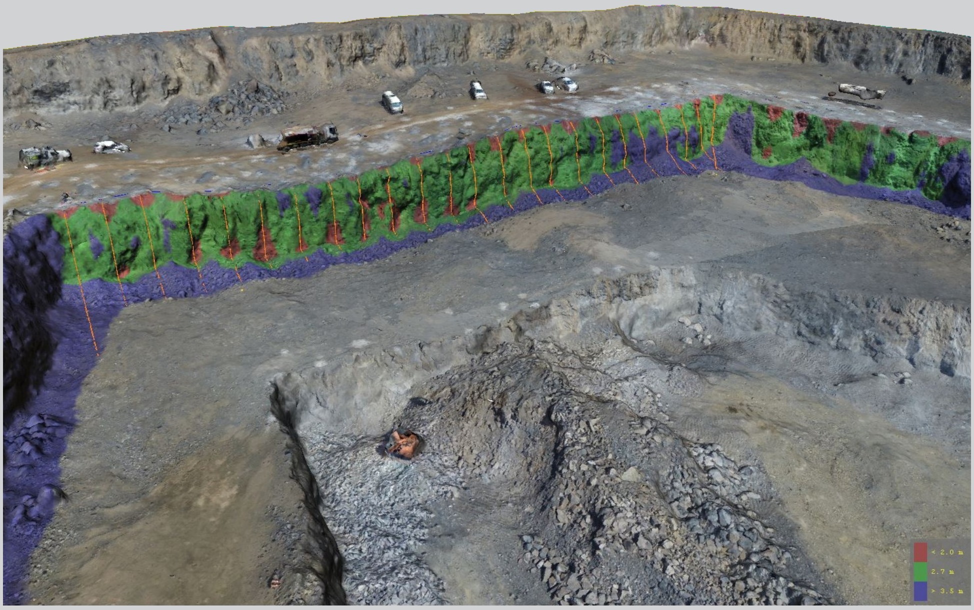

3D images from drones are a perfect survey of large blast sites. Poor blasting results are often caused by inaccuracy of the front row hole placement and suboptimal blast pattern geometry.

Features

- Face profiles (burden diagrams and maps)
- Volume to blast
- Pre-post blast comparison
- Quantification of muckpile (movement, volume, swell)
- Power trough
- Seamless data flow

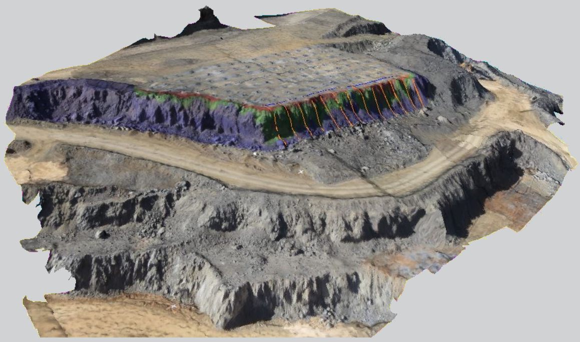

3GSM
Software & Measurement
3GSM.at

3GSM GmbH
8010 Graz - Austria
office@3gsm.at - www.3GSM.at

Promotional article

Ready-to-use satellite based subsidence detection of geo-hazards, infrastructure and mining sites.

Active mining processes can cause seismic activity, negatively affecting communities and infrastructure. Satellite monitoring can identify subsidence and structural defects that are otherwise undetectable, as AS Datel's recently launched SILLE service demonstrates.

AS Datel launched SILLE, an early warning and structural health monitoring e-service in April last year. The early warning system uses data from European Union satellites to detect the shifts and subsidence of infrastructure such as bridges, pipelines, port areas, mines and large buildings with a precision of up to 1 mm. This innovative service helps to prevent accidents caused by deterioration of infrastructure and thus contributes to the general safety of society.

SILLE made the monitoring of technical conditions of infrastructure accessible and financially feasible even for medium-sized companies and organizations. It can be used, for example to detect deformation hazards and carry out structural subsidence analyses and surveys for buildings on unstable ground, such as above clay or underground mines. All of this is carried out by automatic algorithms and the results are regularly verified by experts and by comparison with on-site measurements.

Correct interpretation of information collected from space is extremely research-intensive. In order to achieve highly reliable results, Datel cooperated with universities from several continents.

Data is currently collected from two European Space Agency (ESA) Sentinel satellites, which use interferometric synthetic aperture radar (InSAR) to detect surface movements with an accuracy of a few millimeters, but the service is built in a way that allows for use of additional data sources as well.

InSAR is an active remote-sensing technology that emits microwave impulses towards the ground, with the satellite sensor registering all those that are backscattered or returned.

Sille can be used to monitor objects that reflect well, such as hard surfaces like rocks, artificial objects, metal etc. Suitable objects include buildings, railways, bridges, bare land, etc.

The two Sentinel satellites work in tandem to collect new data for each ground location globally at an interval of six to 12 days, and results are constantly correlated with artificial reflectors on a test polygon to make sure that all calculations are correct.

To collect and calculate deformation data, the satellite emits a radar wave targeted to a structure on Earth and the phase is measured. During the next satellite pass, the process is repeated and a new phase is measured. Then the difference between the two phases is calculated and the difference is found, to enable identification of any deformation.

SILLE benefits:

- Systematic monitoring of large or small areas
- Coverage of the entire world
- It works in all weather conditions
- Giving early warning by monitoring and evaluating safety risks that emerge slowly and cannot be seen with visual inspection
- Indicating places where additional inspections should be carried out
- High accuracy measurement comparable to geodetics
- Survey wide areas without a tripod
- Subscription based service - pay per use
- Applicable to all stages of construction - planning, construction, operation
- After a failure or structural problem, data can show the reasons it occurred and prove that prevention was impossible
- Parallel historic and modern displacement for a broad understanding of local ground subsidence
- Minimize cost of community distrust and physical damage

Sille offers a proactive tool for structural integrity monitoring and disaster prevention. In addition to identifying if surrounding construction, mining, or geological subsidence has caused deformation or structural weaknesses, the service also allows users to develop a timeline for existing subsidence related issues, including data that land or structural deformities pre-existed construction or mining work.

Sille's data can bolster transparency in the mining industry by assessing land and surrounding structures

before and after mining to detect possible movement. This data can also be used as evidence to show that mining has in fact not caused any damages.

The examples below identify the advantage of utilizing the service preemptively to identify movement as soon as it occurs.

CASE STUDY, Chelm Slaski mining area

Poland mines millions of tons of coal every year accounting for just over half of the country's energy consumption. Active mining processes in some areas have caused seismic activity, negatively affecting communities and infrastructure. The majority of coalmines are located in the Silesia region of southern Poland. Bytom and Chełm Śląski are towns less than 50km apart located in the coal basin.

Both have experienced widespread subsidence causing building and road breaks, railway track movements, and resident displacement. Many residents in Bytom have seen their homes and community buildings diminish in value due to mining damages and subsequent repairs. Often repairs do not restore the character of buildings as seen in Image 1.

Mining induced earthquakes were commonplace in Bytom five years ago resulting mostly in mild tremors, according to Earthquake-Report.com. However, in 2011 a serious quake forced an evacuation of 600 people and injured several miners. Most recently, Reuters reported in May 2018 that a 3.5-4.0 earthquake caused a coalmine tunnel to collapse in southern Poland resulting in the deaths of at least two miners and several more trapped almost a kilometer underground.

Image 1. Bytom façade repairs before (top) & after (bottom)

Sille Analysis.

Reconstruction of Bytom and Chełm Śląski deformation indicates a long-term trend with some areas severely sinking. On Image 2 a large cluster of deformation can be seen on the western side of the analysis area, while directly east there is an area of upward movement indicated in blue.

A sharp decline in the Earth's surface can be seen in Image 3 toward the end of 2017, though an ongoing negative trend is clear. A trend of negative deformation can be seen in Image 4 in the red and yellow areas, though some upward movement can be seen in the southwestern corner. A localized analysis of an area in Image 5 shows a neighborhood settling from 2015 to 2018.

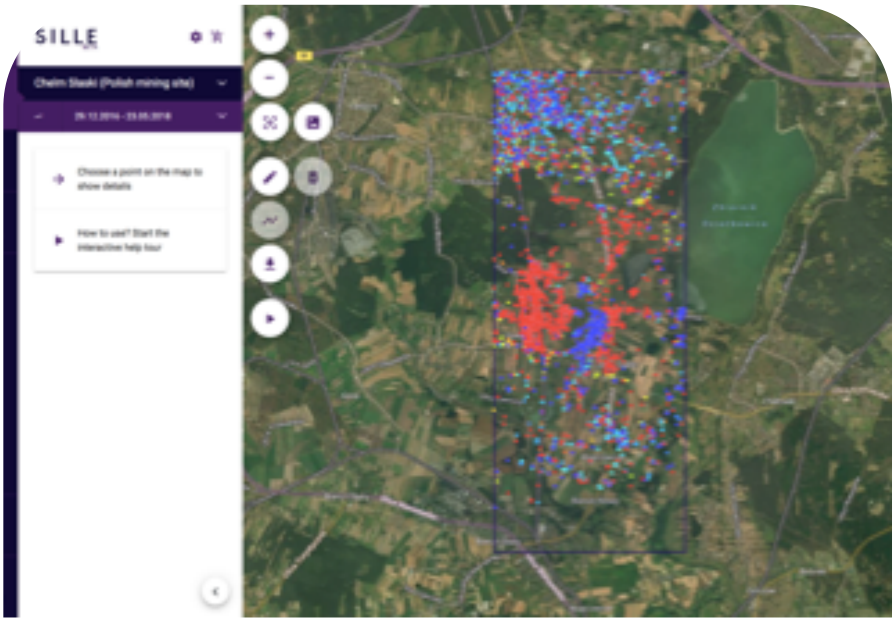

Image 2. Chełm Śląski

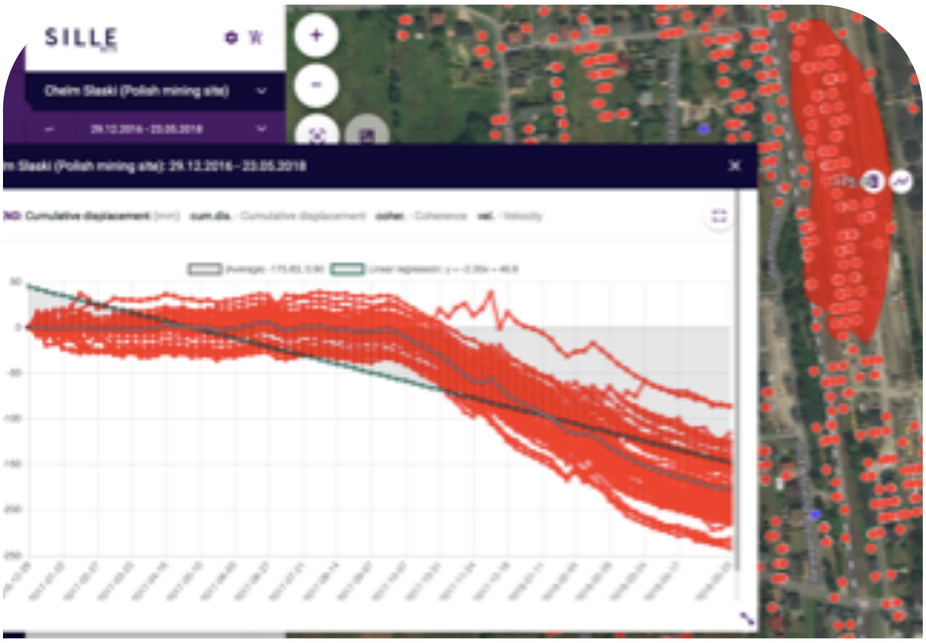

Image 3: Chełm Śląski deformation graphed

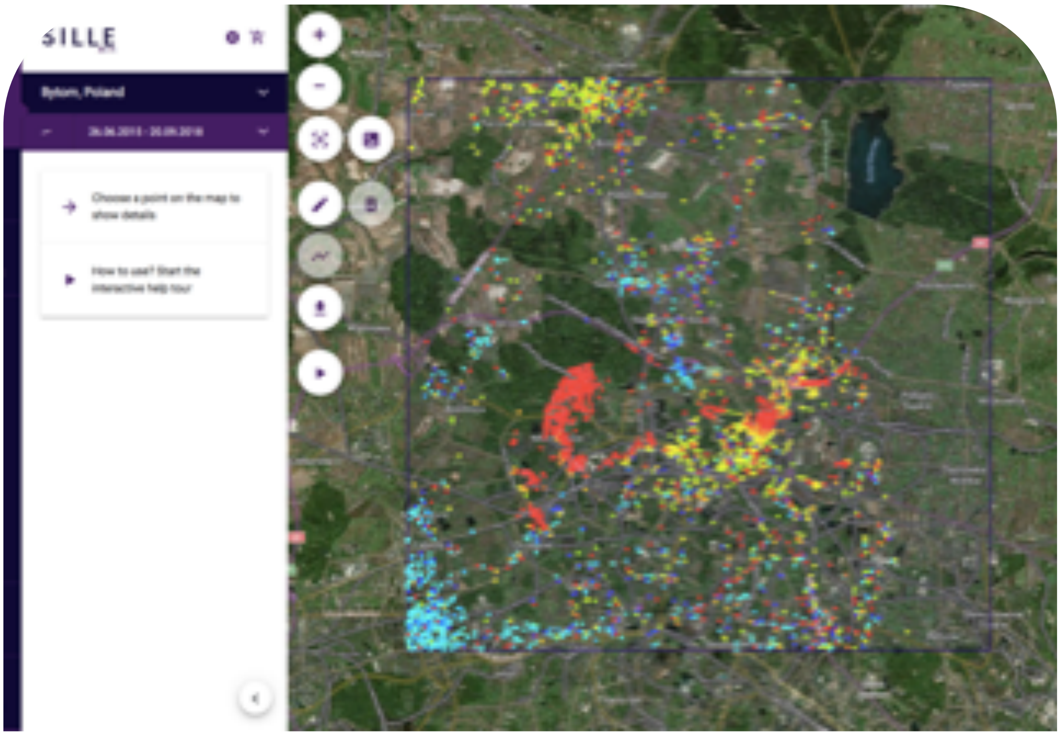

Image 4. Bytom

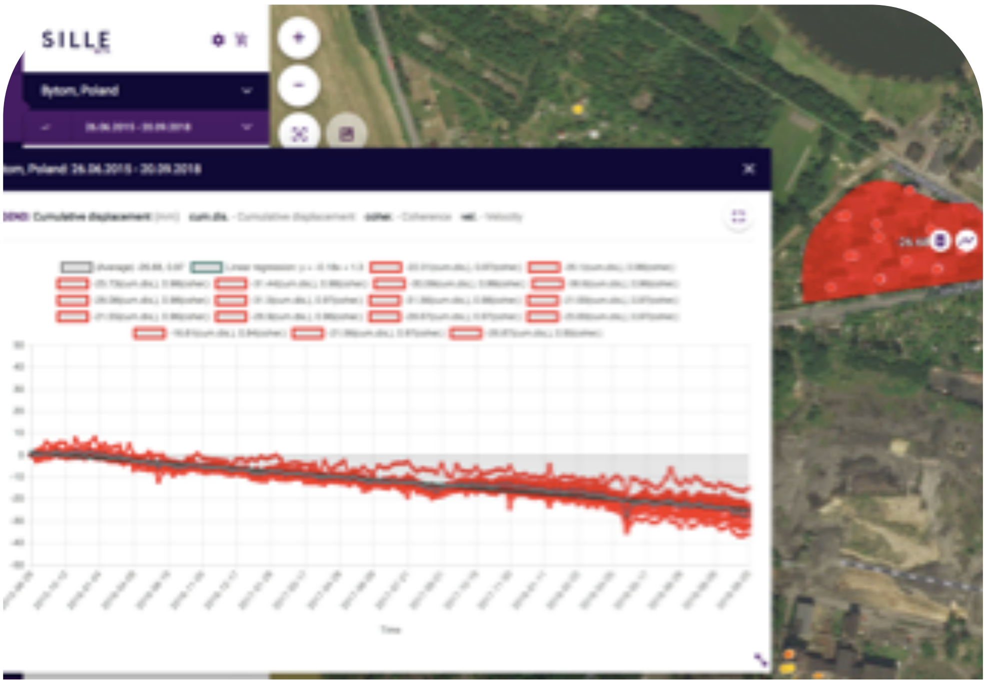

Image 5. Bytom neighborhood settling

CASE STUDY, Rattlesnake Hills Landslide

Background

In late 2017 ground disturbances were noticed above a quarry in the Rattlesnake Hills of Yakima County in central Washington, causing a slow moving landslide. The landslide resulted in a precautionary but indefinite road closure, immediate evacuation due to imminent danger for a neighborhood of around 70 people south of the affected area, multiple crisis contingency plans including the slide's impact on the nearby Yakima River, and actively tasked resources of over 10 local, state and federal agencies. The economic impact of the slide seemed to compound as reports indicated that in addition to the quarry and state both hiring independent consultants to further study the slide, the quarry parent company offered five paid weeks in a hotel for displaced residents.

Technical Background

Quarry mining operations were halted once the vulnerabilities were identified and close monitoring of the area began, including installation of more than 50 GPS monitors, four seismometers, aerial imagery, and terrestrial LiDAR, among others. Efforts were also taken to physically block the landslide.

In May 2018 the landslide, approximately 8 hectares (20 acres) in size, was estimated to be moving at a rate of 45 centimeters (1.5 feet) per week, according to the **Washington State Department of Natural Resources**[1]. **The Seattle Times**[2] reported in June 2018 that the landslide was still being monitored though it had slowed movement indicating that it could be coming to an end. It was estimated that eventually the landslide would contain itself after enough rocks and debris collect into the quarry below.

Sille Advantage

Through displacement reconstruction, InSAR data shows the emerging safety risk of Rattlesnake Hills beginning in 2015 and steadily continuing into 2018. Satellite data shows dramatic negative displacement on the western-facing side of Rattlesnake Hills, consistent with the identified landslide.

Had SILLE been implemented into the scope of monitoring this quarry, its weekly scans would have revealed the effects of the mine early enough to spur precautionary measures allowing time to minimize the landslide's risk to residents.

The value of SILLE is clearly seen in its ability to establish **subsidence history** and **systematically monitor** any size area **without in-situ equipment**.

The service compliments existing analysis techniques to provide a comprehensive look at surface displacement and structural shifts. Within the application users are able to collect, analyze, store, and export data, allowing for multidimensional use.

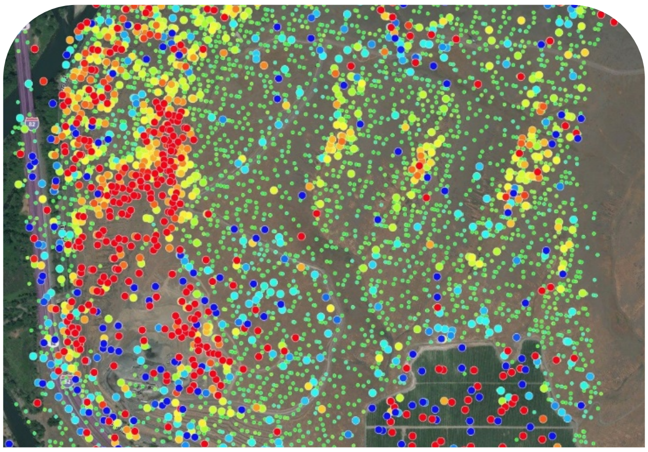

Figure 1. SILLE analysis of Rattlesnake Hills landslide.

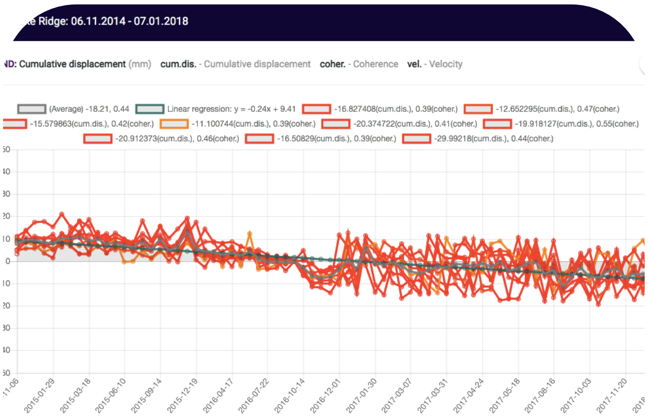

Figure 2. Graphed points of deformation from landslide area.

Figure 3. Image of Rattlesnake Hills before ground shifts. (Google Earth, 2017)

Figure 4. January 2018 image of Rattlesnake Hills. (Tyler Newton, 2018, http://tnewton.com/rattlesnake-ridge-deployment/)

BACK TO TOP

SILLE Risk & Resource Savings

- **Improve understanding of timeline and reasons for occurrence**
- **Implement preventative measures to avoid crisis**
- **Analyze historical displacement for better prediction of future trends**
- **Minimize costs of corrective efforts**
- **Maintain positive public opinion by circumventing potential disaster**

Although the monitoring process can be divided into three main stages – planning, construction and operation – the main applications of the system are in the planning and operation stages. For example, the surface of a building area before construction, ensuring that it is not subsiding or rising and giving evidence to a geological situation.

Meanwhile, during operation, the following can be monitored:

- structures on slopes that can be affected by landslides, collapses and flowing water
- structures close to construction activities where large amounts of soil are dug
- structures with burst or leaking water pipes, where soils are being eroded under the foundation
- **structures located near active mining and blasting work areas**
- old structures that can become dangerous as a result of material degradation
- structures located on or near earthquake zones that are most likely to collapse in the event of seismic activity
- structures damaged after an earthquake that may not be visible to the naked eye
- structures located near sinkholes
- new structures that need regular monitoring to guarantee proper repairs and identify dangerous building errors
- high structures that must be stable, such as masts and tall buildings
- structures with foundation repairs, to make sure that these are correct and they are now stable, or if not, where additional work is needed
- structures insured for full risk, where it is possible to prevent costly repairs caused by deformation damage
- structures on soft soil, landfills, temporarily wet or flooded soils and anything else that can lead to a structure becoming unstable
- structures that are insured, to make certain the deformation damage was evident before making the insurance contract or before buying
- structures at risk of subsidence or other damage where a better overview of risks can help owners avoid costly repairs

- previous constructions by bidders for public tenders, to assess the quality of their work and whether it is structurally damaged
- historical structures such as old castles, manors or churches
- structures where dangerous activities take place, such as nuclear or chemical plants

More information about the Early warning system SILLE can be found at https://www.sille.space

And FB page https://www.facebook.com/sillespace

Asse Hang
VP International Sales
asse.hang@datel.ee

Influence of distorted blast hole patterns on fragmentation as well as roughness of and blast damage behind remaining bench face in model scale blasting

ABSTRACT

This paper describes model-scale bench blasts on mortar blocks with distorted drill hole patterns, done in 2013-2014 at the Montanuniversitaet Leoben. The main aim of the project is to see if the fragmentation from and the crack development behind blasts with and without drillhole deviations differ significantly.

The dimensions of the test blocks were 660×280×210 mm (L×W×H). They were mounted inside a yoke that allows the blast waves escape. Three rows in each block were shot row by row with a nominal pattern of B×S = 70×95 mm. The same nominal delay 73 µs between holes was used throughout. Apart from reference blocks, blocks with holes with stochastic collar position errors (variations in burden and in burden and spacing but constant row volume) and systematically shifted collar positions (blasts with staggered pattern) were shot.

Apart from the sieving analysis, the remaining bench faces have been measured with a stereo-photogrammetric method and linear roughness profiles for each row have been constructed. Sawing slabs from block remains after the 3rd row and use of dye penetrant has allowed the construction of AutoCAD models of the internal blast damage.

Apart from the sieving analysis, the remaining bench faces have been measured with a stereo-photogrammetric method and linear roughness profiles for each row have been constructed. Sawing slabs from block remains after the 3rd row and use of dye penetrant has allowed the construction of AutoCAD models of the internal blast damage.

Preliminary analysis indicates that none of the changes in bore hole collaring have had a significant effect on the sieving curve (median). The sieving results confirm earlier findings though that the fragmentation gets finer with the number of rows shot, implying that blast damage from earlier rows has an influence on the blasting results.

The manuscript will include an updated fragmentation analysis and ongoing work to correlate the roughness and internal damage data to the fragmentation results.

INTRODUCTION

Drilling and blasting are two important parts in quarry production operations. Ineffective blasting, arising from drillhole deviations, may significantly affect, both technically and economically, the overall performance of the process. The larger the drillhole deviation, the larger or smaller the practical burden may become. For high benches the difference between the theoretical and the practical burden values may become substantial (Olofsson, 1988). The back break on the remaining wall is another issue, associated with the drillhole deviations (Konya & Walter, 1991). As a result of an excessive burden, back break may occur, thereby causing the explosive to break and crack the rock behind the last row of holes.

A recent study conducted at a quarry and platinum mine in South Africa (Sellers, Kotze & Mthalane, 2013) measured the effect of drilling accuracy on fragmentation. Drillhole deviations were measured and the fragmentation was evaluated by means of Split Desktop software, based on manually retouched images. The Split results were given in terms of mean (characteristic) fragment size, denoted x_c and n. The study indicated that there was a significant improvement in both x_c and in n when drillhole deviations are reduced, the mean decreased from 242.3 mm to 188.5 mm and n increased 0.89 to 1.24. These results formulas are at variance with the Kuz-Ram model. Ouchterlony (2015) reanalysed Sellers data and found that the Rosin-Rammler curve is a poor descriptor of their sieving curves and gives spurious variations in n. Using the truncated Rosin-Rammler distribution, which has also a top fragment size parameter x_{max} , the curve fits in the fines and coarse ranges improve considerably. More importantly, while the improved drilling decreases the characteristic fragment size x_c from 238 to 187 mm, or x_{50} from 177 to 143 mm, the n-value hardly changes at all, it increases only slightly from 0.86 to 0.91.So we have two contradicting experiences:

- The Kuz-Ram model and Lownds who predict that n but not x_{50}, (or x_c) is influenced by drill hole deviations
- Sellers, Kotze & Mthalane (2013) reinterpreted findings that the deviations influence x_{50} and x_c but hardly n.

In addition the suggestion that n should increase by 10% if the drilling pattern is staggered should be also investigated.

In order to investigate how drillhole deviations influence fragmentation, small-scale blasting tests have been carried out with the same methodology as used by Johansson and Ouchterlony (2013) and Schimek, Ouchterlony & Moser (2013). Three different drillhole deviation patterns and one staggered pattern were used to investigate the matter of fragmentation. In addition the effects of drillhole pattern on face roughness and blast damage behind the blasted rows were measured.

Two test series were conducted, 2013 and 2014. In the first blocks with two different sets of stochastic collaring errors in the burden direction were compared with reference blocks without collaring error. In the second blocks with stochastic collaring errors in both burden and spacing direction and blocks with an staggered drilling pattern, a systematic distortion, were compared with reference blocks.

1. TEST SET UP

The small scale tests on magnetic mortar blocks were conducted at a blast site, owned by Montanuniversiaet Leoben (MUL) and located at the Erzberg iron mine, 30 km north of Leoben. The mortar is well defined and a similar composition has given repeatable fragmentation results in rock blasting tests (Johansson et al. 2008; Johansson & Ouchterlony 2013; Schimek et al. 2013).

Test blocks mounted inside an inner yoke, made from high strength concrete inside the outer yoke were used (see FIG 1). The gap between the inner yoke and the outer yoke was filled with compacted sand, which transmitted about 70% of energy of the blasting waves into the surrounding yoke (Maierhofer 2011).

Figure 1 –Yokes at the Erzberg blasting site. They allow waves to escape from a test specimen. The inner yoke has room for the block.

At the sides and at the back, the test block was grouted into the inner yoke by using fast hardening cement, which had similar material properties as the blocks, minimizing the impedance difference. During the tests the area within the wire fence was covered with rubber mats and heavy non-woven felt to trap the blast fragments.

The basic ingredients and proportions of the magnetite concrete can be seen in TABLE 1.

From TABLE 1 a difference can be seen in water content and in the grain size of the quartz sand used in 2013, compared to the one in 2014. For production 2014, additional 8 l water was added to the recipe, for a complete hydration of the concrete.

To check the blastability of the different batches of mortar several cylinders with a diameter of 138.5 mm and a height of 280 mm have been produced from each batch. These cylinders were blasted with a 20 g/m detonating cord in a 10 mm diameter blasthole and a sieving analysis was done as a measure of the repeatability of the fragmentation properties.

Test session	2013	2014
Ingredient	[%]	[%]
Portlandcement CEM II / A-M 42.5 N	25.60	25.60
Water	12.65	12.65*
Glenium 361 (Plasticizer)	0.26	0.26
DCC- Defoamer	0.13	0.13
Magnetite powder (Ferroxon 618)	29.65	29.65
Quartz sand 0.1 - 0.5 mm (ME 31)	31.70	-
Quartz sand 0.1 - 0.4 mm (ME 01-04)	-	31.70

*Additional 8l water was added for the 2014 production

TABLE 1. Ingredients of the magnetite concrete blocks

Testing blocks

The dimensions of the testing blocks used for blasting were 660x280x210 mm (LxHxW), the same as Johansson & Ouchterlony (2013) used. The blastholes with a diameter of 10 mm were through going and drilled in the laboratory using core-drilling equipment. The arrangement of all blocks was 3 rows per block, 7 boreholes per row, all vertical. The spacing and the burden were 95 mm and 70 mm, giving S/B ratio of 1.36. The bottoms of the blocks were resting on a piece of conveyor belt. Angled holes were not used, firstly because they are difficult to drill and secondly because it was believed that a straight hole with the same collaring error as the bottom deviation of an angled hole with perfect collaring would have larger effect on the fragmentation.

Explosives and delay time used

The nominal delay between the holes was chosen to be 73 µs or 1.0 milliseconds per meter (ms/m) of burden, long enough to avoid shock wave interactions between neighbouring holes and short enough to avoid large scale tearing effects. This delay was achieved by using a 5 g/m detonating cord, lying in loops on a piece of a conveyor belt. This arrangement was used to protect the yoke from the detonation of the delay-timing cord. The blasting was done by using a 20 g/m detonating cord and was thus top initiated. All the shots started from the right side and proceeded to left for all three rows.

Drill patterns blast session 2013

For the session 2013 variations in the spacing were eliminated, because the Kuz-Ram model implies that a variation in spacing on average does not influence the specific charge and thus neither x_{50}. The influence on n would not even out as the average fragment size distribution of two blast parts with different specific charge values but the same n would be flatter and hence have a lower n-value. Systematic variations in the burden might however show up as variation in local specific charge, which influences x_{50}. Thus the design used boreholes with random row-wise uncorrelated variations in the burden. The following design steps were undertaken:

1. The normal, rectangular drill pattern was used as a reference.
2. A series of 200 pseudo random numbers in the range (-1.1) was taken and 13 sequences of 7 consecutive numbers with an average per set within ±0.025 were selected.
3. The 13 sequences were matched against each other and pairs with an inter-row correlation factor |r| < 0.01 were chosen.
4. A combination of three sequences with very low inter-row correlation, forming a near stochastic pattern, was chosen to give the collaring error in the burden direction.
5. The combination number 13-7-3 refers to one of these sequences 13 (row 1), 7 (row 2) and 3 (row 3) respectively. Adding the geometrical positions of the holes upwards (larger burden) with the holes downwards (smaller burden), the result is always near zero (within ±0.025), thus a near constant breakage volume, and hence average specific charge per row was achieved.
6. The maximum deviation from the straight line was chosen to be 25 mm, comparable to the one in Sellers, Kotze & Mthalane (2013) in terms of standard deviation, relative to burden SD/B=0.638*25/70=0.23. Thus according to the Kuz–Ram model, n ∝ (1-SD/B) should decrease by about 25%.
7. Two combinations of random drillhole deviation patterns were tested: combination 13-7-3 (1st burden deviation) and combination 2-3-7 (2nd burden deviation). See FIG 3.

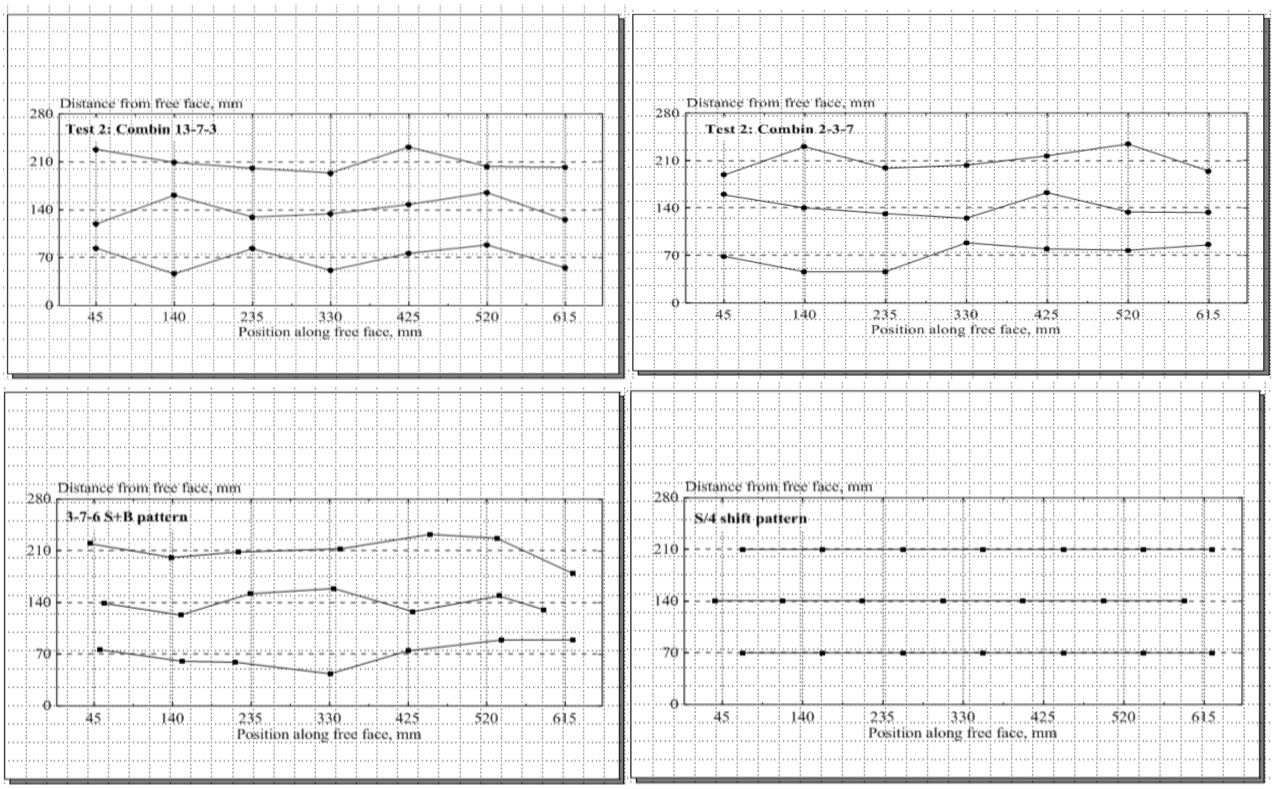

FIG 3 –Drilhole deviation patterns: Top 2013: 13-7-3 (1st burden variation) left and 2-3-7 (2nd burden variation) right; Bottom 2014: 3-7-6 (S+B deviations) left and S/4 shift right

Deviation patterns blast session 2014

For the blast session 2014, two new designs were introduced: stochastic collaring errors in both the spacing and burden (B+S variations), and systematic collaring errors only in spacing (±S/4 shift) i.e. a staggered pattern.

The following design steps were taken to create the burden and spacing variations:

1. The same rectangular drilling pattern was used as a reference.
2. Two columns of 250 random uniform variables, with a correlation factor $|r| < 0.01$ to use as Δx and Δy generators for variations in spacing (x) and burden (y) directions, were taken.
3. Applying the Box-Muller method (Box & Muller, 1958), two columns of normally distributed numbers with mean 0 and variance of 0.75 were calculated. The numbers followed the bivariate normal distribution well.
4. Working with two independent parameters at the same time made it harder to meet the same criteria as for the burden only variation of 2013. Seven sequences of paired numbers were found for which: 1) $|\text{mean}(\Delta x)| < 0{,}2$ and $|\text{mean}(\Delta y)| < 0{,}1$, 2) $|\text{corr.}(\Delta x, \Delta y)| < 0.2$ and 3) $|\text{stdev}(\Delta x)-\text{stdev}(\Delta y)| < 0{,}2$.
5. For all pairs of sequences, the Δx and Δy, the Δx with Δx and Δy with Δy correlations were calculated. Those for which both $|\text{corr.}| < 0.4$ were accepted as neighbouring rows of collaring errors.
6. An amplification factor λ = 20 mm (see below) was chosen such that $\Delta S = \lambda \cdot \Delta x$ defined the collaring error in the S-direction and $\Delta B = \lambda \cdot \Delta y$ the error in the B-direction. This corresponds to a drilling deviation SD/B of about 0,15 or the same as Sellers, Kotze & Mthalane (2013) case of normal drilling
7. The blasting patterns were plotted, and burdens and edge hole positions were checked.

The starting and final bull's eye diagrams for (Δx, Δy) are shown in FIG 2.

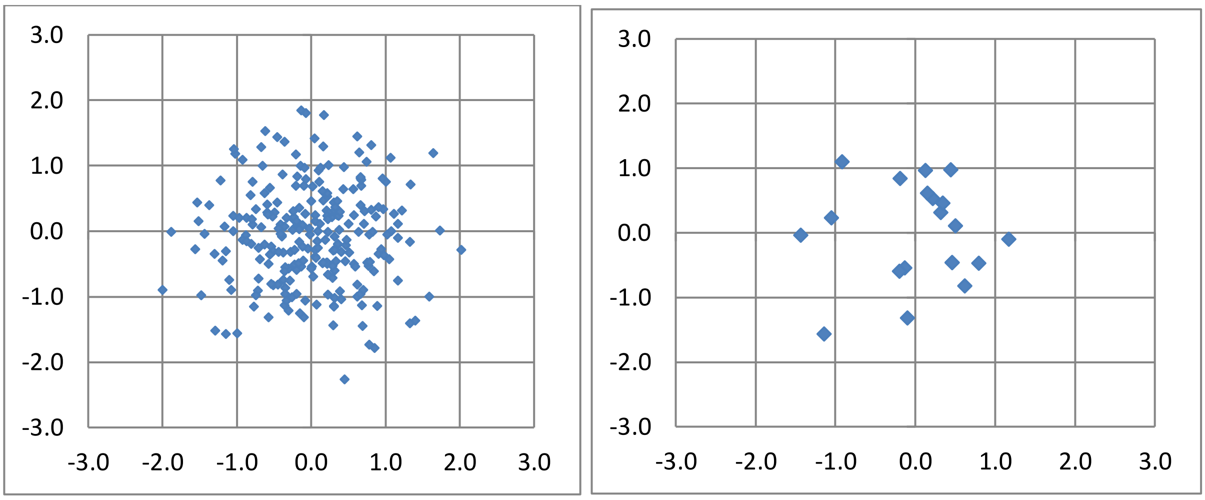

FIG 2 –Bull's eye diagrams: 250 Box-Muller pairs (Δx, Δy) (left) and finally chosen 21 values (right)

As a result of the described above design set up, the following criteria were met:

1. Blasting pattern with almost uncorrelated collaring errors ΔS and ΔB;
2. Blasting pattern with nearly uncorrelated collaring errors between rows;
3. Blasting pattern with nearly same average burden volume for each row and as a consequence nearly the same nominal specific charge;
4. Blasting patterns where collaring errors in burden and spacing directions can be tested separately or together;

The second design for the blast session 2014 was an staggered pattern, created by shifting the hole collaring positions in each row sideway by+ S/4 in the first row, -S/4 in the second row and +S/4 in the third row to minimize edge effects in the block.

FIG 3 (see above) shows the drillhole deviation patterns selected for the blast sessions 2013 and 2014.

Sieving analysis and data evaluation

After each blast, the blasted material was collected and a sieving analysis was done. The sieving was done as follows (Grasedieck, 2006): The grains of the coarser material were analysed individually by sticking them through the mesh of the sieves. The sieves used for that procedure were: 125; 100; 80; 63; 50; 40; 31.5; 25; 20; 14; 12.5; 10 mm. The finer material was sieved by hand using the screen sizes: 6.3; 4; 2; 1; 0.5; mm.

The sieving data were presented as cumulative distribution function (CDF) curves of mass passing vs. mesh size x and specific percentile x-values x_{30}, x_{50} and x_{80} corresponding to mass passing at 30 %, 50 % and 80 % were interpolated linearly.

The Swebrec distribution (Ouchterlony 2005, 2009) was used as a fitting function because it gives better fits than most other functions (Sanchidrián et al. 2009, 2012). In addition, from the sieving curves the equivalent n-values were calculated.

Investigation of blast induced damage

Investigation on blast induced damage was done by measuring the surface roughness of the bench face after blasting and the crack development behind shots with drillhole deviation and reference shots (shots without drillhole deviations). The procedures are briefly described below.

Analysis of surface roughness

After each row blast, the bench contour/surface was photographed with a 3D camera system, 3G BlastMetrix (Moser et al. 2006). Out of the pictures with reference delimiters and range poles, 3D-models of the bench faces were computed.

Three horizontal contour lines were taken; at 5, 10 and 15 cm of the block height for the analysis of the under/over break. With help of MATLAB® (by MathWorks, Inc.) the mean distance of the individual data points to the as drilled reference line (D_{Mean}) was calculated as an under/over break parameter. In addition, the normalized slope inclination (S_{Norm}) of the individual sections of the contour lines as a micro-roughness parameter of the bench surface was calculated.

Surface crack detection of the top on testing blocks

During the blast tests of 2014, pictures of the top on the testing blocks were taken after each row blasted (see FIG 4). A dye penetration technique and a 3D digital scale model method were applied for the visualization and assessment of the internal crack damage (Navarro, 2015). The cracks were traced with help of AutoCAD® (by Autodesk, Inc.). A subdivision of rows and corresponding burden was done.

Eleven crack families with regards to their length, angle and origin were recognized. Manual counting of the cracks within each family was done as well as statistical evaluation of the data.

Surface crack detection on cut slices

After the blast tests of the blocks, fast hardening cement was poured in front of the remains of the block behind row 3 to stabilize them so that they could be removed from the yoke and brought to the laboratory. From corresponding horizontal cut slices in those specimens blast-induced cracks were detected by using the same dye penetration technique, (see FIG 5), counted and statistically evaluated.

As a measure of the introduced damage, the mean crack density (MCD) was calculated. For the calculation of MCD, the cut slice was divided into a grid of 2 x2 cm, where the sum of the cracks in the individual cells was divided by the total amount of cells.

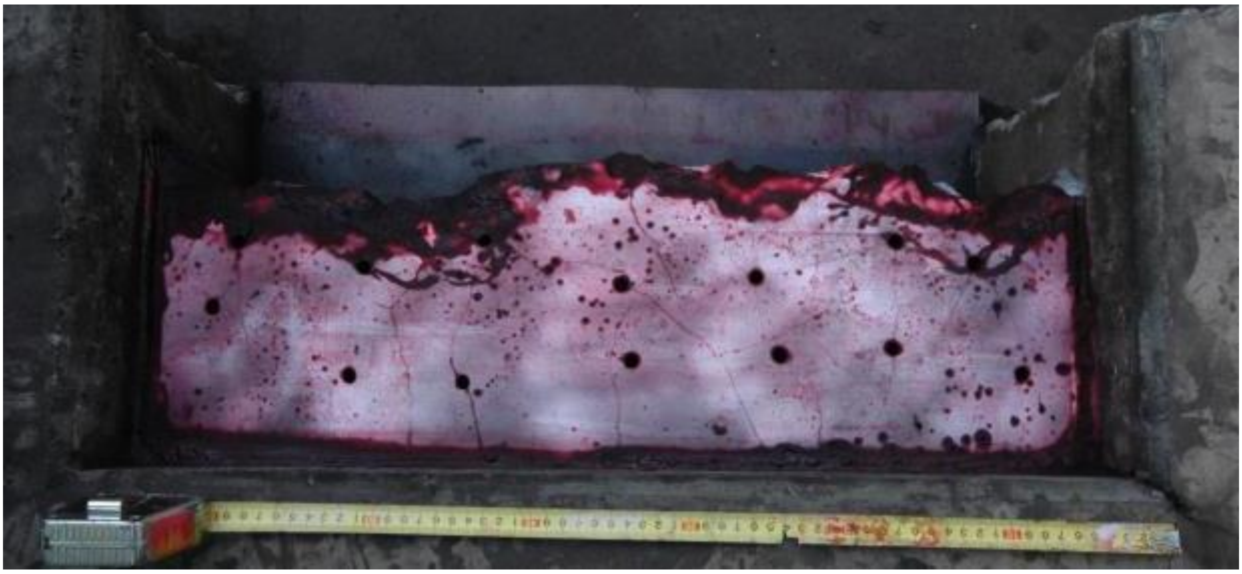

FIG 4 –Surface crack detection of the top of testing blocks

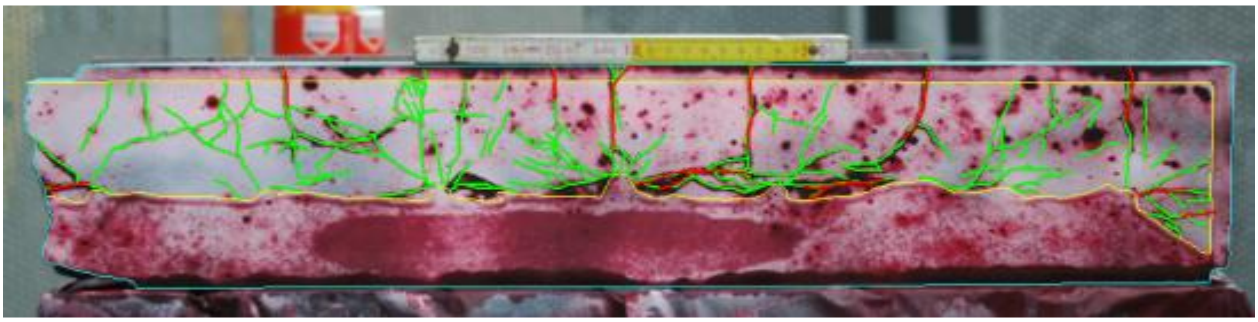

FIG 5 –Surface crack detection in cut slices

2. RESULTS

Material properties

The physical and mechanical properties of Ø50-mm cylindrical core samples from cubes cast from the same batches as the blocks were determined. The aim was to define any factor or variable in the magnetic mortar properties that could effect on fragmentation results. TABLE 2 shows the obtained results.

TABLE 2 shows that the average mortar density from blast session 2014 is 13 % lower than that for 2013. All other data for 2014 are lower than the corresponding data for 2013 except the Poisson's ratio.

TABLE 3 gives a summary of the sieving parameters of the cylinders shots that were made to obtain a measure of the blastability of the mortar batches.

TABLE 3 shows that the sieving parameters for each year have good repeatability between different batches. The average x_{50} for 2014 is 12% lower than for 2013, which can be explained by the changes in the material properties (see TABLE 2). A one-way Anova showed with 95% level of confidence that this difference is significant.

Material property	2013		2014		Unit
	Mean	Stdev	Mean	Stdev	
Density	2.273	10	1.986	35	kg/m³
UCS	58.1	5.5	35.8	4.6	MPa
Brazilian tensile strength	5.52	0.09	3.56	0.56	MPa
Young's modulus	23.9	0.5	14.0	0.9	GPa
Poisson's ratio	0.12	0.01	0.17	0.03	-
P-wave velocity	3756	79	3056	36	m/s
S-wave velocity			1989	36	m/s

TABLE 2. Material properties of mortar core samples

Session	Batch	x_{30} [mm]	x_{50}[mm]	x_{80} [mm]
2013	1	8.43	15.45	24.61
	2	8.78	15.92	26.43
	3	7.97	14.26	22.78
Average		**8.39**	**15.21**	**24.61**
Stdev		**0.41**	**0.86**	**1.83**
2014	1	8.10	13.24	22.23
	1	8.39	13.34	22.05
	2	8.06	13.61	24.43
	2	7.57	13.54	23.32
Average		**8.03**	**13.43**	**23.01**
Stdev		**0.34**	**0.17**	**1.10**

TABLE 3. Sieving parameters of the cylinders

Fragmentation results session 2013

TABLE 4 shows the x-values for the session 2013. The blocks are identified by mortar batch or charge (CH) and block (B) numbers.

The repeatability of the data between block pairs with the same drilling pattern is not very good. The relative difference is worst for row 1 of the reference blocks, 38% and for row 3 of the 1st burden variation, 30%. For all other rows this value lies in the range 6-22%. The average relative difference is 18%, which is going to make it difficult to find any significant effect of the pattern changes that have been made. The equivalent n-values are discussed further in the article.

Block	Row	x_{30} [mm]	x_{50} [mm]	x_{80} [mm]	Equivalent n value ($1.507/\ln(x_{80}/x_{30})$)
CH01B03 (Reference)	1	26.08	57.61	91.35	1.20*
	2	9.94	21.36	73.09	0.76
	3	8.50	17.51	43.12	0.93
CH01B05 (Reference)	1	15.64	32.43	64.29	1.07*
	2	10.41	22.42	54.45	0.91
	3	7.71	14.54	37.00	0.96
CH01B02 (1st burden deviation)	1	13.74	30.14	110.05	0.72*
	2	11.63	23.61	61.67	0.90
	3	10.12	19.95	52.05	0.92
CH01B04 (1st burden deviation)	1	13.56	25.87	84.61	0.82*
	2	9.77	18.96	47.81	0.95
	3	7.53	13.86	33.84	1.00
CH03B01 (2nd burden deviation)	1	16.55	54.42	117.74	0.77*
	2	10.87	25.61	79.76	0.76
	3	8.96	18.09	46.15	0.92
CH03B02 (2nd burden deviation)	1	20.28	44.74	88.13	1.03
	2	9.53	24.53	79.05	0.71
	3	9.78	19.38	55.32	0.87

*Values excluded in analysis, due to a dust and boulders kink in mass passing curve

TABLE4.Sieving parameters blast session 2013

FIG 6 shows the median fragment size data x_{50} from TABLE 4. It can be seen that x_{50} decreases with increasing row number. This is probably an effect of a first preconditioning of the mortar by blasting of the 1st row, which causes back break and radial cracks in the previously intact material, see e.g. Johansson and Ouchterlony (2013) and Schimek, Ouchterlony & Moser (2013). The third row, in turn, undergoes preconditioning of both rows 1 and 2 blasted in respective order. In the photo documentation from DalFarra (2012) and Navarro (2015) it was deduced, that some cracks reaching the third row are generated already from blasting row 1.

The relative variation in the fragmentation in the second and the third row appear to be somewhat smaller, compared to the one in the first row;

The average fragment size for row 1 is with one exception (1st burden deviation), larger than half the nominal burden B/2 = 35 mm; this corresponds to a fragmentation behaviour, which can be described as "dust and boulders", i.e. relatively few large blocks and a fines tail (Ouchterlony & Moser 2013).

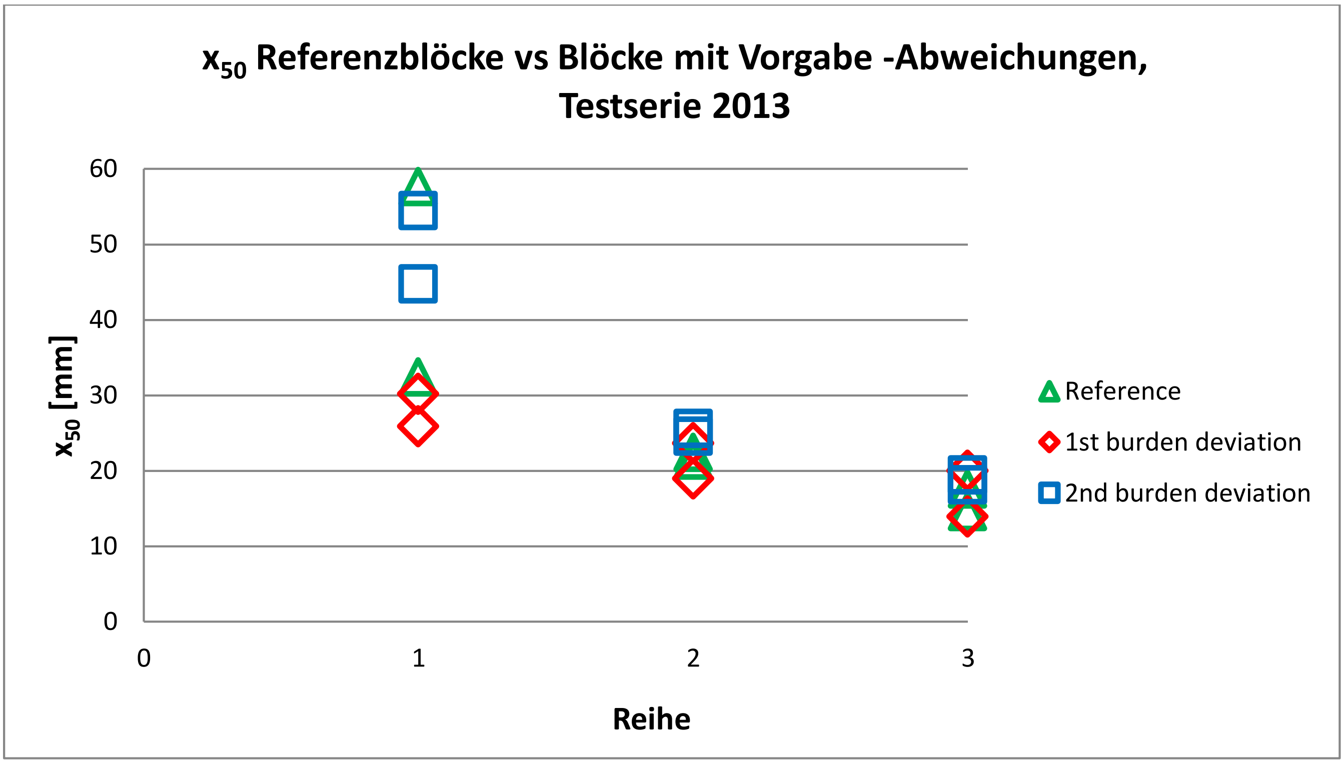

FIG 6 –Median fragment size x50 values plotted row wise for blocks shot in 2013 Referenzblöcker vs Blöcker mit Vorgabe-Abweichungen, Testserie

Similar results were also found by Johansson and Ouchterlony (2013), who linked this mechanism with possible contribution to the large scatter in the 1st row.

FIG 7 shows the result of the sieving analysis of row 1 of block CH01B05 (Reference block), fitted with the Swebrec function and which represents a typical "dust and boulders" behaviour.

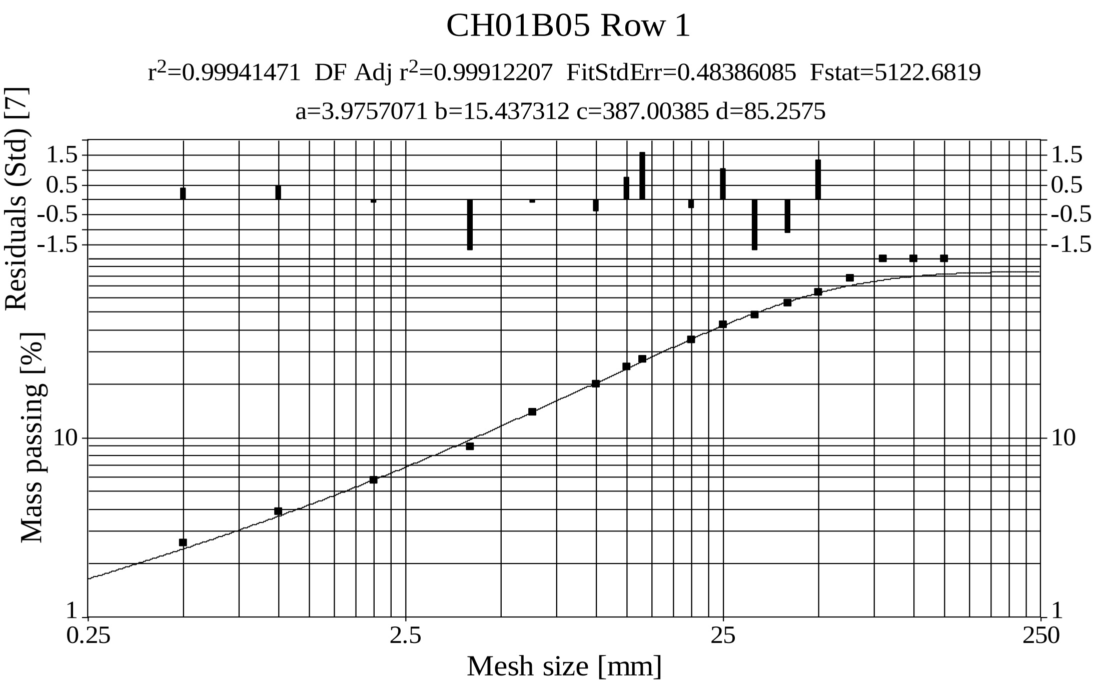

FIG 7 –Sieving curve block CH01B04 (1st burden deviation)

The fines tail is well described by Swebrec function with an amplitude of less than 100 (d = 85%). The large blocks are so few that it becomes difficult to describe the fragmentation by a continuous sieving curve. A better description is a continuous fines tail, with a discrete coarse part added.

The sieving curves of second and third rows were in general very well described by both three and five parameter Swebrec functions with 100% amplitude, i.e. there is much less dust and boulders type fragmentation in these rows. The data for the percentile size values x_{30} in TABLE 4 show pretty much the same behaviour as the x_{50} data, see FIG 8. The x_{80} data show larger variations, see FIG 9.

Anova and Kruskal-Wallis evaluations of the sieving parameters in TABLE 4 were conducted to find out if specific groups are significantly (statistically) different. The result was that with 95% level of confidence there is no significant difference between the means of the groups for x_{80}, x_{50}, x_{30} parameters within rows 1, 2 and 3 respectively. This was one reason why the testing for 2014 used three blocks for each drilling pattern instead of two.

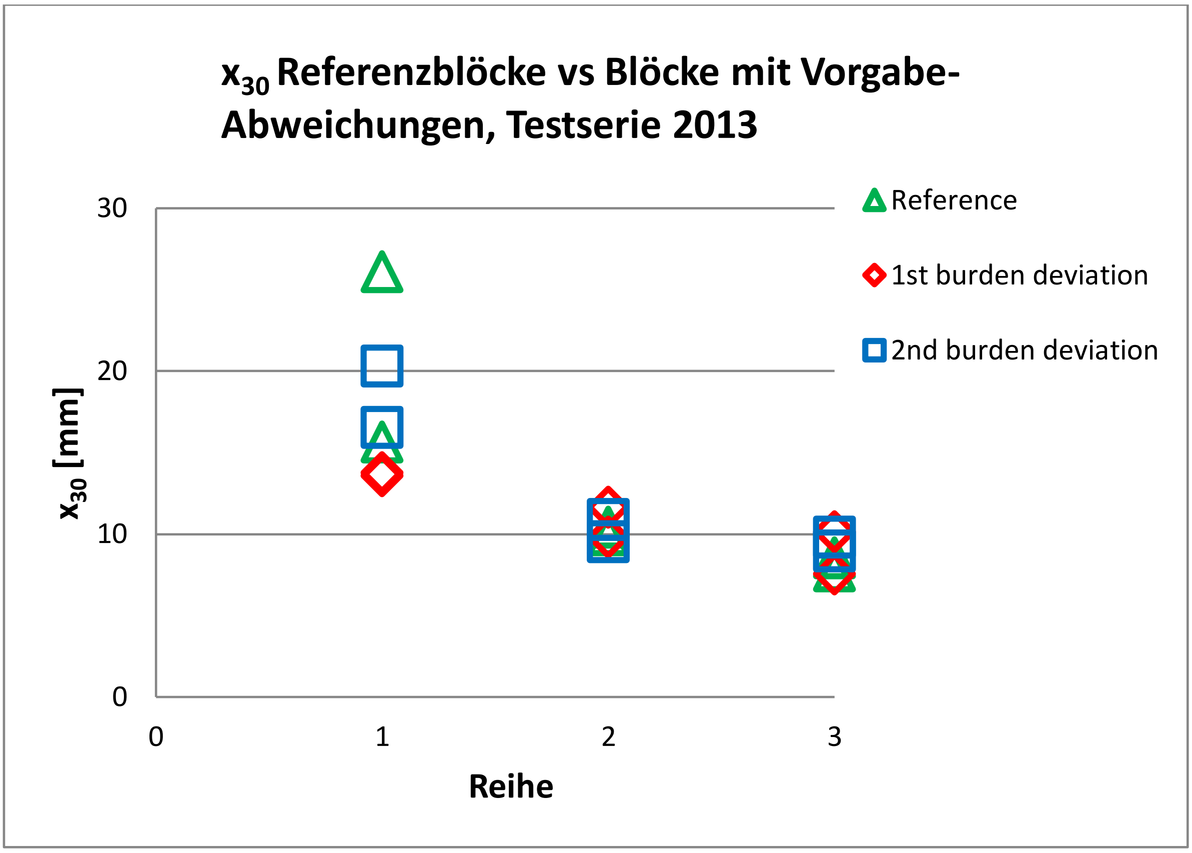

FIG 8 –Percentile size x_{30} values, plotted row wise for blocks shot in 2013

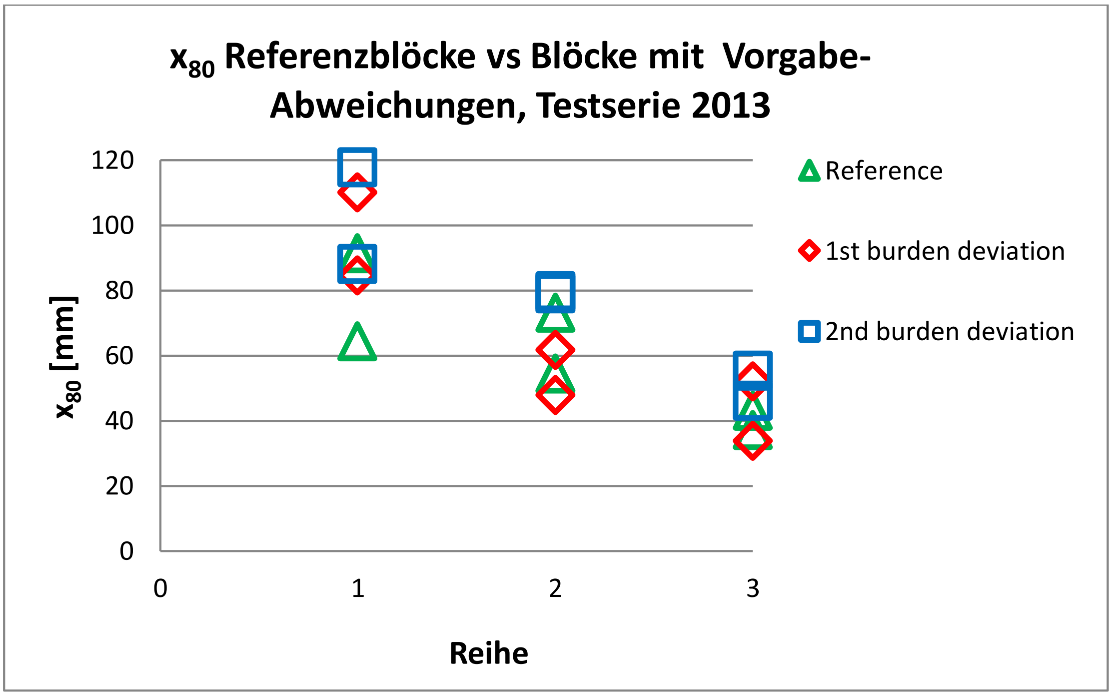

FIG 9 –Percentile size x_{80} values, plotted row wise for blocks shot in 2013

Fragmentation results session 2014

TABLE 5 shows the x-values for the blast session 2014.

The repeatability of the data between block groups (triplets) with the same drilling pattern is still not very good. The coefficient of variation (COV = mean/stdev) is worst for row 1 of the reference blocks, 79% due to the very coarse fragmentation obtained for block B01. Block B01 may be seen as an outlier. For the row 1 shots of the other two patterns the average COV of 39% is nearly twice as large as the average COV for all rows 2 and 3, 23%. Again this is going to make it difficult to find any significant effect of the pattern changes that have been made.

The fragmentation in row 1 was described as often "dust and boulders", i.e. relatively few large blocks and a fines tail. For the second and third row the fragmentation is finer and the scatter is smaller too. FIG 10 gives an example of sieving curve for the third row block B07 (S/4 shift), where it can be seen that the curve is well described by the Swebrec function with amplitude d = 100%.

Block	Row	x_{30} [mm]	x_{50} [mm]	x_{80} [mm]	Equivalent n value (1.507/ln(x_{80}/x_{30})
B01 (Reference)	1	56.96	90.63	>125	
	2	12.28	29.07	67.07	0.89*
	3	9.06	19.63	50.85	0.87*
B06 (Reference)	1	11.34	22.03	48.47	1.04
	2	8.65	18.60	44.07	0.93
	3	5.83	12.61	33.94	0.86
B09 (Reference)	1	16.95	38.05	83.93	0.94
	2	8.07	16.37	39.24	0.95
	3	5.86	12.76	36.44	0.82
B03 (S+B variations)	1	9.41	23.69	71.03	0.75
	2	7.23	16.58	45.86	0.82
	3	9.17	19.25	49.62	0.89
B04 (S+B variations)	1	9.02	20.58	61.30	0.79*
	2	6.30	15.67	53.50	0.70
	3	6.52	13.97	37.48	0.86
B10 (S+B variations)	1	19.07	43.76	103.83	0.89*
	2	11.70	25.58	101.59	0.70
	3	9.44	18.62	42.23	1.01
B02 S/4 shift	1	19.67	46.92	90.01	0.99*
	2	21.64	49.19	89.24	1.06
	3	11.42	22.02	48.24	1.05
B07 S/4 shift	1	30.14	79.13	102.74	1.23*
	2	15.43	39.55	81.46	0.91
	3	8.80	17.80	42.68	0.95
B11 S/4 shift	1	17.83	39.12	90.75	0.93
	2	11.73	28.27	71.78	0.83
	3	10.89	21.49	48.83	1.00

*Values excluded in analysis, due to a dust and boulders kink in mass passing curve

TABLE 5. Sieving parameters blast session 2014

FIGs 11-13 show the percentile size values x_{30}, x_{50} and x_{80} from TABLE 5. The same tendency for the values to decrease with row number as for the 2013 data can be seen for x_{30} and x_{50} but for x_{80} this trend is far from apparent. A general tendency in FIGs 11-13 is that the percentile size values for the staggered pattern tend to be the highest.

The one way Anova test of the sieving parameters showed, that there is no significant difference between the means of the groups for x_{80}, x_{50} and x_{30}, within rows 1, 3 and most of row 2. The only difference between the mean values was found between the x_{50} groups of the S+B variations and the S/4 shift in the 2nd row. The analysis also shows that there is no significant difference between the group means when the data for all patterns are combined.

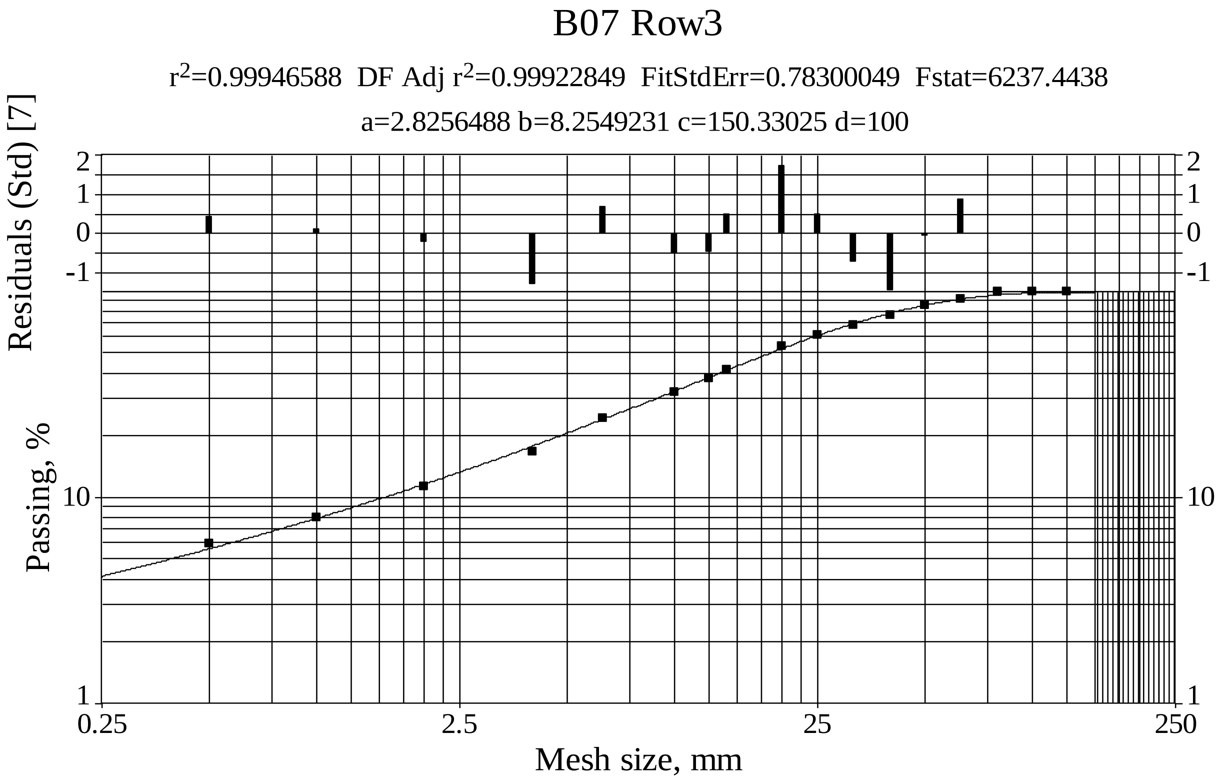

FIG 10 –Sieving curve 3rd row block B07 (S/4 shift)

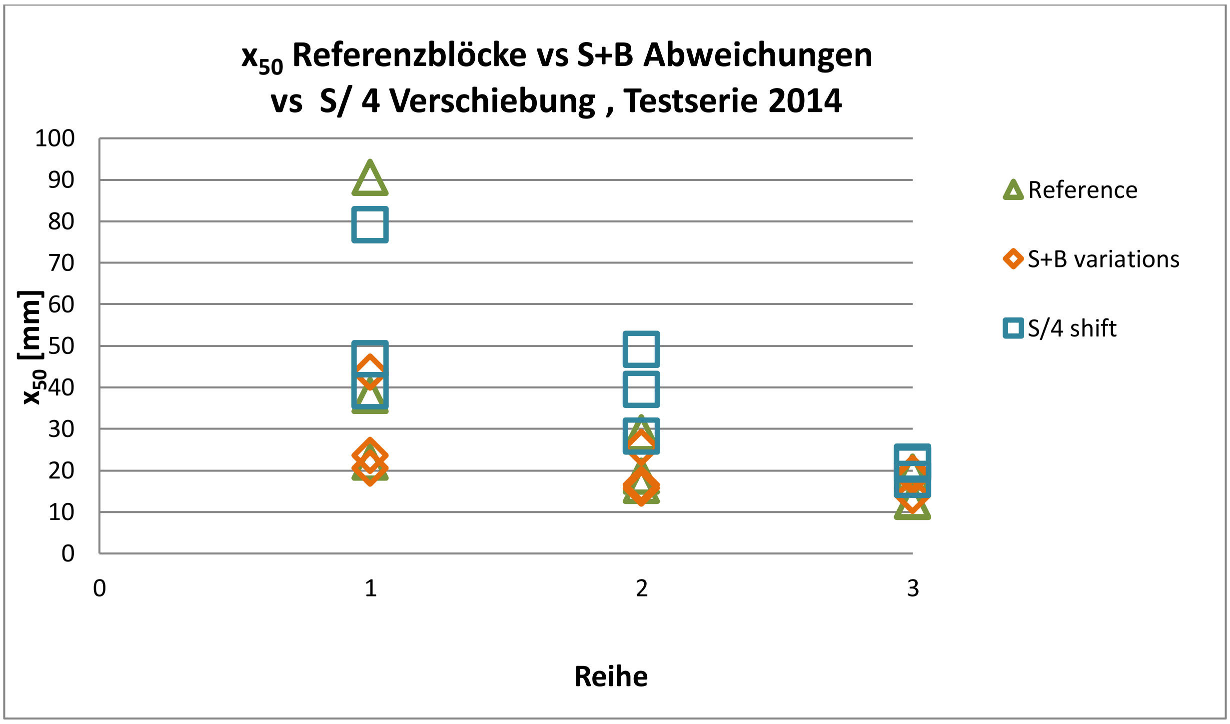

FIG 11 –Median fragment size x_{50} values, plotted row wise for blocks shot in 2014

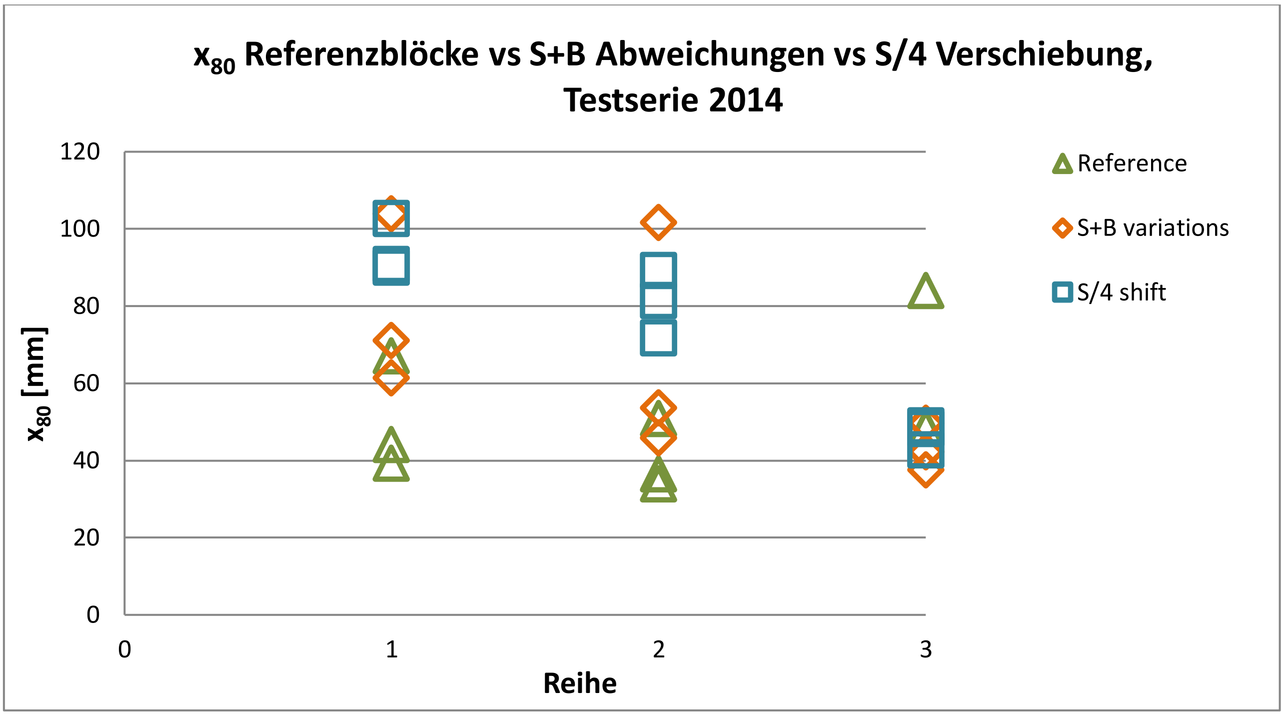

FIG12 –Percentile size x80 values plotted row wise for blocks shot in 2014

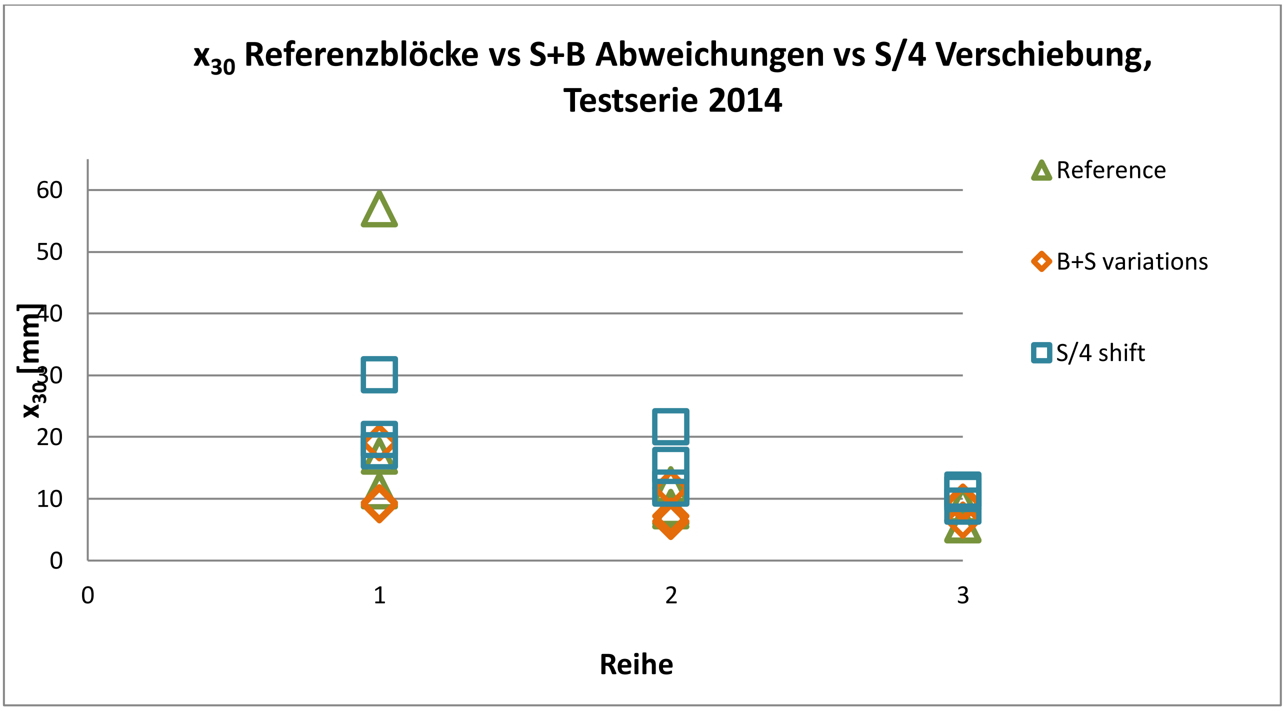

FIG13 –Percentile size x30 values plotted row wise for blocks shot in 2014

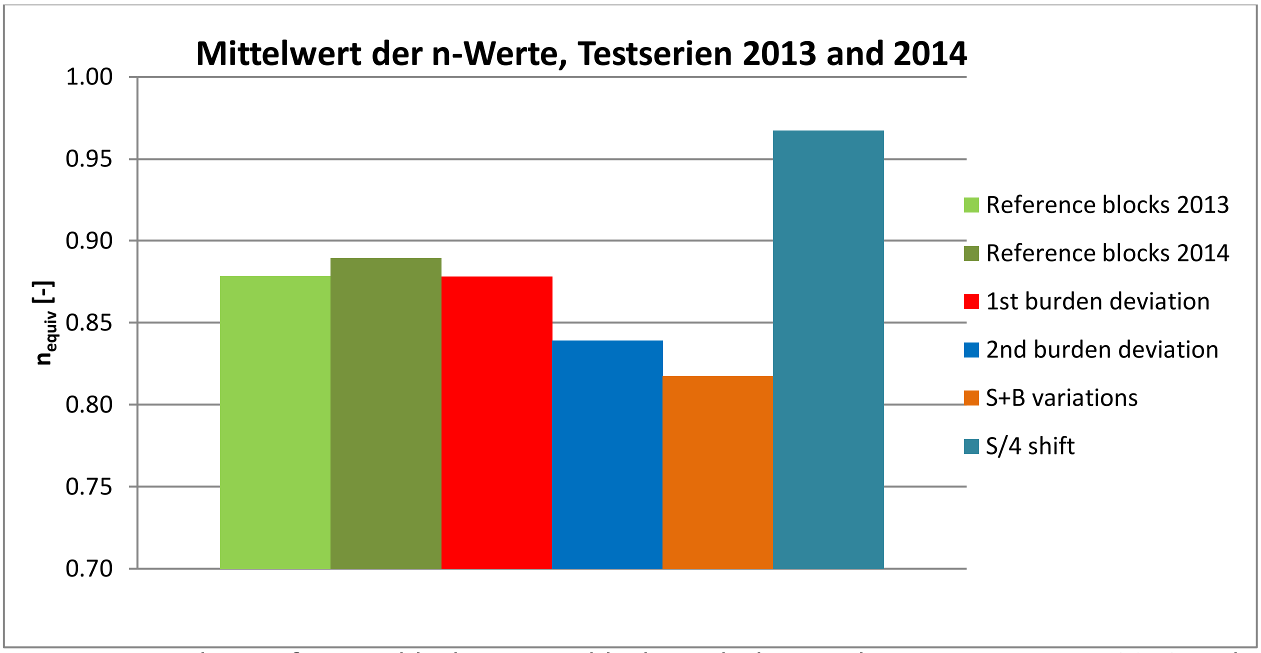

FIG 14 – n- values reference blocks versus blocks with distorted pattern, sessions 2013 and 2013

Equivalent n-values results

From the sieving curves, equivalent n-values were calculated from fitting a Rosin-Rammler function to the x_{30} and x_{80} values in order to see if there are any changes when the distorted patterns were tested. The corresponding equation is $n_{equiv} = 1{,}507/\ln(x_{80}/x_{30})$. For this equivalence to be meaningful, the equivalent x_{50}-value corresponding to the x_{30}-x_{80} fit has to be nearly the same as the interpolated x_{50}-values in TABLEs 4-5. This is mostly not the case when there is a severe dust and boulders effect. Then there is kink in the mass passing curve, see FIG 7, which destroys the agreement between the two x_{50} values. Thus the row 1 data have been checked and some n_{equiv} values judged as invalid, among them the data for outlier block B01. FIG14 gives a summary of the valid n_{equiv} values.

FIG 14 shows the average n-equivalent values for each drill pattern. Similar equivalent n- values in both 2013 and 2014 reference patterns can be seen. The equivalent n-value for the blocks from groups 2nd burden deviation is a decrease as for the 1st burden deviation data this trend is no apparent.

A general tendency in FIG 14 is that the equivalent n- values for the staggered pattern tend to be the highest and the S+B variations the lowest.

The S/4 shift pattern showed 10% higher n-value, compared to the reference pattern, while the S+B variations pattern with uncorrelated collaring errors ΔS and ΔB in S and B directions respectively has shown a 7% decrease in the n-value.

The one way Anova test of the equivalent n-values showed, that there is no significant difference between the means of the groups for Reference blocks, 1st and 2nd deviation pattern blocks. The only significant difference between the mean n_{equiv} values was found between the Reference, S+B variations and the S/4 shift. The analysis also shows that there was significant difference between the group means when the data for all patterns in 2014 are combined.

Surface roughness results

FIG 15 shows a box and whisker plot of the roughness data with means and indicated outliers, where each plot is based on three horizontal contour lines at 5, 10 and 15 cm of the block height, for the 1st, 2nd and 3rd row respectively.

A general tendency is that the surfaces for the staggered pattern tend to be the smoothest. However, the surface of the rest of the blocks with both reference and distorted patterns showed no clear trend of larger or smaller overbreak, see FIG 15.

Regarding the roughness surfaces in rows, the measured D_{mean} (except 2nd burden deviation pattern) showed a tendency to increase from the first to the second row blast while for the third row a tendency to decrease was seen; i. e the largest backbreak was observed in the second row.

The normalized slope inclination S_{norm} of the surface showed for the shots in 2014 a tendency to increase from the first to the second row blast, and to decrease for the third row. For the 2013 shots no such trends could be seen.

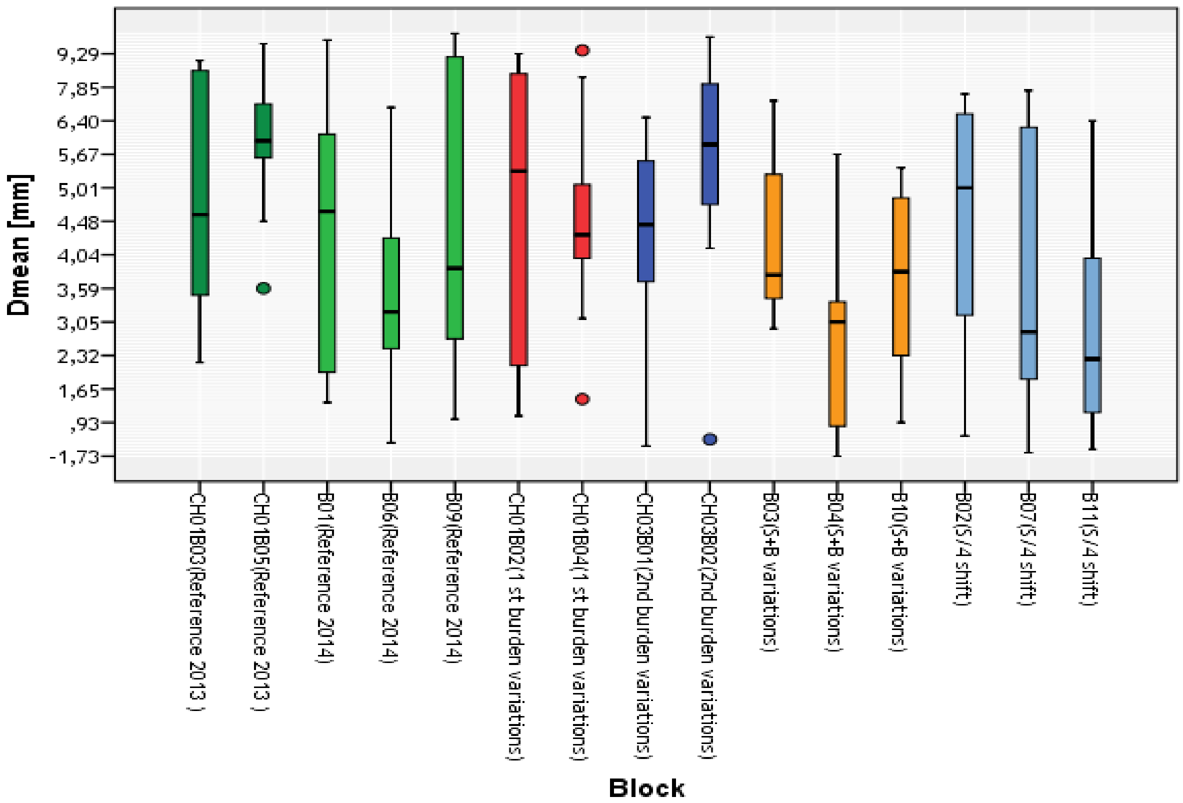

FIG 15 –Box- Whisker plot over the surface roughness Dmean for different drill patterns

Crack detection results

The investigations of the crack development on cut surfaces indicated that out of the eleven detected crack families four tend to be most influenced by blasting: radial cracks directed to the boreholes in sectors 80^0-30^0 and 30^0-0^0, plus near surface connection cracks between boreholes and internal cracks parallel to the surface. It was also detected that the number of cracks varies the cutting height of the slices. Judged by the calculated average mean crack density (MCD) it was found that the reference blocks from 2013 were more damaged than the reference blocks from 2014.

For the session 2013, a high MCD value was found for the 1st burden deviation pattern, while for the 2nd burden deviation pattern the MCD value was the

lowest. Remains from blocks with the staggered pattern from 2014 were found to be less damaged than those from the blocks with the reference pattern.

The documentation pictures of testing blocks as well as at the surface crack detection of the top of testing blocks supported these results. A detailed crack detection analysis is still under way.

SUMMARY OF EXPERIENCES

A series of small scale tests were conducted to investigate the effect of drillhole deviations on fragmentation. The experimental set-up simulated bench blasting and it was designed to minimize any geological influences as well as to minimize the side effect from wave reflection.

Different material properties were observed for sessions 2013 and 2014, due to the changes in the ingredient properties, this must be taken into account by comparing blasting results from sessions 2013 and 2014.

With regards to fragmentation, we have experienced the following:

- When shooting in intact material (row #1) the scatter is large and the fragmentation is coarse, showing "dust and boulders" behaviour.
- For the second and third row, the scatter is smaller, the fragmentation is finer and the sieving curves follow the Swebrec function well. It means that blast damage from previous rows improves the fragmentation and may help to decrease the scatter in the fragmentation results in subsequent rows.
- For the session 2013, where burden deviation patterns were tested, the arrangement in terms of standard deviation, relative to burden SD/B = 0.23, was according to the Kuz–Ram prediction model expected to lower the n-value by about 25%.
- The statistical analysis of the data for session 2013 showed with 95% confidence, that the fragmentation of all 6 blocks is essentially the same, neither x_{50} nor n are significantly influenced by the burden variations.
- The statistical analysis of the data for session 2014 showed with 95% confidence, that all for 9 blocks x_{50} values are essentially the same, while the equivalent n-values the analysis showed that for S/4 shift and S+B deviations patterns these values are significantly different.
- The tests demonstrated that the equivalent n-value n_{equiv} has increased 10% by shooting staggered pattern. This finding corresponds well with the literature (Cunningham, 1983).

- The S+B variations showed that the percentile size values x_{30}, x_{50} and x_{80} were not significantly different The n_{equiv}-value decreased by 7% however and the statistical evaluation showed that this difference was significant. This decrease is about half of the around 15% predicted by the Kuz-Ram model.
- The surface roughness investigation indicated that a smooth surface was achieved by the staggered, S/4 shifted pattern. The other deviations patterns did not show a clear trend.
- For all patterns except 2nd burden deviation pattern, the highest D_{mean} values were found in the second row blasts, i.e. a larger backbreak occurred in the second row compared to in the first and third rows.
- The D_{mean} and S_{norm} parameters chosen to describe the surface roughness seem to give good description on the blasted surface. With the surface roughness, it was expected that introducing of drillhole deviation the backbreak on the remaining wall would increase and for the reference blocks it would be less pronounced. However looking to the mean values of the individual blocks there was no clear trend detected.
- The smooth surface, achieved with the staggered or S/4 shifted pattern together with the amount of damage introduces by cracks, may explain why the staggered pattern gave a somewhat coarser fragmentation.
- The damage has been measured in the remaining part of blocks. It was found that four crack families seemed to be most affected by blasting, while the other families were not as much affected. The comparison of the reference and staggered patterns showed that less cracks were apparent for the staggered pattern, i.e. less damage was introduced.

With respect to the high scatter in the data no firm conclusions can be drawn to answer if drillhole deviation affects the fragmentation. The results could be interpreted in two ways: there is no effect on burden variations under our conditions, or the effect of the burden variations is hidden by the repeatability variations of our tests. The data is still under evaluation, including further analysis to gain a final statement. More data should help to give more conclusive answers.

R Ivanova[1], F Ouchterlony[2] and P Moser[3]

1. Research Assistant, Chair of Mining Engineering, Montanuniversitaet Leoben, Franz-Josef-Strasse 18, 8700 Leoben, Austria, e-mail: radoslava.ivanova@unileoben.ac.at

2. Senior Scientist, Chair of Mining Engineering, Montanuniversitaet Leoben, Franz-Josef-Strasse 18, 8700 Leoben, Austria, e-mail: finn.ouchterlony@unileoben.ac.at

3. Head of Chair, Chair of Mining Engineering, Montanuniversitaet Leoben, Franz-Josef-Strasse 18, 8700 Leoben, Austria, e-mail: peter.moser@unileoben.ac.at

ACKNOWLEDGEMENTS

The colleagues at Swedish Blasting Research Centre at Luleå University of Technology, where the setting with the same set up started are highly acknowledged. The authors would also like to acknowledge the work of Juan Navarro and Clara Villaro Mores for their MSc thesis work that contributed to this work. Thomas Seidl is also thanked for his work with algorithms ofr surface roughness calculations. Finally, we would like to thank Gerold Wölfler and Georg Glatz for their continuous efforts during the blasting experiments.

This article was originally published in 2015 in Proc of 11 th Int Symposium on Rock Fragmentation by Blasting, Sydney (Fragblast 11 conference, Sydney). We would like to thank to original publisher 11 th Int Symposium on Rock Fragmentation by Blasting for allowing us re-publishing of the article in EFEE proceeding.

REFERENCES

Box, G and Muller, M, 1958. A Note on the Generation of Random Normal Deviates, *The Annals of Mathematical Statistics,* 29, (2), pp 610–611.

Cunningham, C V B, 1983. The Kuz-Ram model for prediction of fragmentation from blasting. *In Proc 1st Int Symp on Rock Fragmentation by Blasting,* (eds: R Holmberg & A Rustan), Luleå University of Technology, Sweden, pp 439-453.

Cunningham, C V B, 1987. Fragmentation estimations and the Kuz-Ram model – four years on. *In Proc 2nd Int Symp on Rock Fragmentation by Blasting,* (eds: W L Fourney & R D Dick), pp 475-487.

Cunningham, C V B, 2005. The Kuz-Ram fragmentation model – 20 years on. *In Proc 3rd EFEE World Conf on Explosives and Blasting,* (ed: R Holmberg), EFEE, UK, pp 201-210.

Dal Farra, E, 2012. Initiation delay effects on fragmentation and face geometry in small-scale blasting tests. Master Thesis, Politecnico di Torino.

Giltner S & Koski A, 2010. The application of a blast audit for production improvement. In *Proc of 9th Int Symp on Rock Fragmentation by Blasting* (ed: J A Sanchidrián), pp 723-730, (Taylor & Francis Group, London).

Grasedieck, A, 2006. Die natürliche Bruchcharakteristik (NBC) von Gesteinen in der Sprengtechnik, Doctoral Thesis, Montanuniversitaet Leoben, Chair of Mining Engineering and Mineral Economics.

Johansson, D, Ouchterlony, F, Edin, J, Martinsson, L & Nyberg, U, 2008. Blasting against confinement, fragmentation and compaction in model scale. *MassMin 2008 – Proc of 5th Int. Conference & Exhibition on Mass Mining*. (eds: H Schunnesson & E Nordlund) pp 681–690.

Johansson, D & Ouchterlony, F, 2013. Shock wave interactions in rock blasting: the use of short delays to improve fragmentation in model-scale, *In Int J Rock Mech and Rock Eng,* 46(1):1-18.

Konya, C and Walter, E, 1991. Rock Blasting and Overbreak Control. *McClean, VA: United States Department of Transportation Federal Highway Administration*, pp 190-192.

Lownds, C, 1983. Computer modelling of fragmentation from an array of shotholes. *In Proc of 1st Int Symp on Rock Fragmentation by Blasting.* (eds: R Holmberg & A Rustan) pp 455-468.

Maierhofer, E, 2011. Development of a blasting area and blasting tests with concrete blocks in half scale to research different fragmentation phenomena, Master thesis, Montanuniversitaet Leoben, Chair of Mining Engineering and Mineral Economics.

Moser, P, Gaich, A, Zechmann, E, and Grasedieck, A, 2006. The SMX Blast Metrix – A new tool to determine the geometrical parameters of a blast based on 3D imaging. In Proc *of 9th Int Symp on Rock Fragmentation by Blasting, Santiago 7-11 May* pp 80-84.

Navarro, J, 2015. Quantification of blast-induced cracks, Master thesis, Montanuniversitaet Leoben, Chair of Mining Engineering and Mineral Economics.

Nielsen K and Kristiansen J, 1996. Blasting- Crushing-Grinding: Optimisation of an Integrated Comminution System. *In Proc of 5th Int Symp of Fragmentation by Blasting,* (ed: B Mohanty) pp 269-277.

Olofsson, S, 1988, Applied explosives technology for construction and mining, *Published by APPLEX S-64043, ÄRLA, Sweden.*

Olsen V, 2009 Rock quarrying: Prediction Models and Blasting Safety. Doctoral Thesis, Norwegian University of Science and Technology.

Ouchterlony, F, 2005. The Swebrec function: linking fragmentation by blasting and crushing. *Mining Technology (Trans. Inst. Min. Metall. A) 114: A29-A44*.

Ouchterlony, F, 2009. Fragmentation characterization; The Swebrec function and its use in blast engineering, *Rock Fragmentation by Blasting, In Proc of 9th International Symposium on Rock Fragmentation by Blasting*, (Ed: J A Sanchidrián), pp 3–22, (Taylor & Francis Group: London).

Ouchterlony, F & Moser, P, 2013. On the branching-merging mechanism during dynamic crack growth as a major source of fines in rock blasting.*In Proc Int Symp of 10th Rock Fragmentation by Blasting*,(Fla CRC Press/Balkema), p. 65-75.

Ouchterlony, F, 2015. The median versus the mean fragment size and other issues with the Kuz-Ram model, *Rock Fragmentation by Blasting, Proc of 11 th Int Symposium on Rock Fragmentation by Blasting*, Sydney (Manuscript submitted to Fragblast 11 conference, Sydney).

Rosin, P & E Rammler, 1933. The laws governing fineness of powdered coal. *Journal of the Institute of Fuel, vol 7*, pp 29-36.

Sanchidrián, J A, Segarra, P, López, L M & Ouchterlony, F, 2009. Evaluation of some distribution functions for describing rock fragmentation data, in Proc Fragblast 9, Proc 9th Int Symp On Rock Fragmentation by Blasting (ed: J A Sanchidrián), pp 239-248 (Taylor & Francis Group: London).

Sanchidrián, J A, Ouchterlony, F, Moser, P, Segarra, P & Lopéz, L, 2012. Performance of some distributions to describe rock fragmentation data, In J Rock Mech Min Sci, 53:18-31.

Schimek, P, Ouchterlony, F & Moser, P, 2013. Experimental blast fragmentation research in model-scale bench blasts, *in Workshop hosted by Fragblast 10 – Measurement and Analysis of Blast Fragmentation* (eds: J A Sanchidrián & A K Singh), pp 51-60 (CRC Press, Taylor & Francis Group: London).

Sellers E, Kotze M & Mthalane, 2013. Quantification of the effect of inaccurate drilling on the risk of poor fragmentation and increased blast hazard*. In Proc of 10 th Int Symp on Rock Fragmentation by Blasting*, (ed: P K Singh & A Sinha), pp 153-161.

45th annual ISEE Conference on Explosives and Blasting Technique in Nashville

EFEE representatives were present for the 45th annual ISEE conference in Nashville, Tennessee in January.

This year the explosives engineering event gathered a record number of participants of 1819 attendees and 187 exhibitors in the Gaylord Opryland resort and convention centre. Participants arrived in Nashville from all over the states of USA and numerous other countries from around the world.

The Gaylord resort and convention centre, where the conference has been held numerous of times, is equivalent to a small indoor town with thousands of hotel rooms, shops, restaurants, walkaways, channels with boat cruises, water amusement park etc. The convention centre itself is able to carry not only one but several large conferences, with attendees in thousands, simultaneously. Close to the Gaylord lies the famous Grand Ole Opry, where country music legends play live 4 time a week. The largest shopping mall of Nashville is merely a 5-minute walk from the Gaylord centre. Well worth a trip is the Nashville city centre, which is reached by taxi in 20 minutes. There the main theme is Country and Western, both as museums and live acts.

Importantly Nashville is also the home of a world class ice hockey team, the Nashville Predators, which is worth a visit if music and malts are not your main thing.

During the conference there were interesting technical presentations run in two large lecture rooms simultaneously. Apart from attending several of the many interesting presentations the EFEE representatives also managed to attend and contribute to the Welcome Reception, the International Luncheon and the Seismograph Section meeting. Furthermore, we had the pleasure of talking to the new ISEE president James P. Daley.

The large tradeshows and exhibition were assembled one floor down from the presentations. It was difficult to comprehend that the event was visited by close to 2000 people because they were spread in several enormous halls and the only time it felt crowded was when free conference lunch was served in the exhibition area. The three conference days and two exhibition days left nicely room to get acquainted with everything.

We enjoyed the 45th ISEE conference in Nashville where we had a chance to meet and exchange news with hundreds of old and several new business acquaintances. We were pleased to get confirmation from many top technical delegates, recognized authors and major international exhibitors that they were committed to join the upcoming anniversary, the 10th EFEE world Conference on Explosives and Blasting which will be held in Helsinki on the 15th - 18th of September 2019.

The next ISEE conference will be held in Denver 26-29th of January 2020 and we are looking forward to once again join this great event.

Johan Gjødvad, Roger Holmberg and Jari Honkanen, EFEE

New EFEE Members

EFEE likes to welcome the following members who recently have joined EFEE.

Individual Members

Darren Francis, Newcrest Mining Limited , Australia

Corporate Members

HANWHA Corporation, South Korea

Upcoming International Events

WORLD TUNNEL CONGRESS
2019 May 3-9, 2019
Naples, Italy
www.wtc2019.com/

UNDERGROUND CONSTRUCTION PRAGUE 2019 (UC PRAGUE 2019)
June 3-5, 2019
Prague, Czech Republic
www.ucprague.com

Europyro 2019 / 44th International Pyrotechnics Society
June, 3-7, 2019
Tours, France
www.europyro2019.org

EFEE 10th World Conference on Explosives and Blasting
September 17-19, 2019
Helsinki, Finland
www.efee2019.com/

WORLD TUNNEL CONGRESS 2020
May, 15-21, 2020
Kuala Lumpur, Malaysia
www.seacetus2017.com/4/443/welcome-to-malaysia/

50. Internationale Tagung für Sprengtechnik
November 7 – 8, 2019
Place: WIFI Linz, Austria
Official language: German
Website/Contact info regarding the conference: www.wifi-ooe.at

Upcoming National Events

Bergdagarna
March 19-20, 2019
Place: Münchenbryggeriet, Stockholm
Official language: Swedish (foreign presentations in English)
Website/Contact info regarding the conference:
http://www.svbergteknik.se

41. Informationstagung Sprengtechnik
April 26-27, 2019
Place: Siegen
Official language: German
Website/Contact info regarding the conference:
www.sprengverband.de

Blasting technique 2019
May 22 – 24, 2019
Place: Hotel Academia, Stará Lesná, Slovakia
Official language: Slovak (foreign presentations in English)
Website/Contact info regarding the conference: www.sstvp.sk

Informationstagung für Bohr-, Spreng- und Ankertechnik
Place: CAMPUS SURSEE Bildungszentrum Bau, CH-6210 Sursee LU, Switzerland Date: 13. / 14. September 2019
Official language: German
Website/Contact info regarding the conference:
www.sprengverband.ch

Blasting technique and pyrotechnics 2019
September 25 – 27, 2019
Place: Hotel Valeč, Czech Republic
Official language: Czech (foreign presentations in English)
Website/Contact info regarding the conference: www.sttp.cz